Synchrony and perturbation transmission in trophic metacommunities

Pierre Quévreux, Matthieu Barbier, Michel Loreau

Synchrony and perturbation transmission in trophic metacommunities

Pierre Quévreux[1], Matthieu Barbier[1], and Michel Loreau[1]

[1] *Theoretical and Experimental Ecology Station, CNRS UMR 5321, 09200 Moulis, France*

corresponding author: pierre.quevreux@cri-paris.org

Key words

food chain, top-down, bottom-up, dispersal, coupling, biomass distribution

Abstract

In a world where natural habitats are ever more fragmented, the dynamics of metacommunities are essential to properly understand species responses to perturbations. If species' populations fluctuate asynchronously, the risk of their simultaneous extinction is low, thus reducing the species' regional extinction risk. However, identifying synchronising or desynchronising mechanisms in systems containing several species and when perturbations affect multiple species is challenging. We propose a metacommunity model consisting of two food chains connected by dispersal to study the transmission of small perturbations affecting populations in the vicinity of an equilibrium. In spite of the complex responses produced by such a system, two elements enable us to understand the key processes that rule the synchrony between populations: (1) knowing which species have the strongest response to perturbations and (2) the relative importance of dispersal processes compared with local dynamics for each species. We show that perturbing a species in one patch can lead to asynchrony between patches if the perturbed species is not the most affected by dispersal. The synchrony patterns of rare species are the most sensitive to the relative strength of dispersal to demographic processes, thus making biomass distribution critical to understand the response of trophic metacommunities to perturbations. We further partition the effect of each perturbation on species synchrony when perturbations affect multiple trophic levels. Our approach allows disentangling and predicting the responses of simple trophic metacommunities to perturbations, thus providing a theoretical foundation for future studies considering more complex spatial ecological systems.

Introduction

Biodiversity is under increasing anthropic perturbations that alter populations and community dynamics (*e.g.* the latest IPBES assessment (Díaz et al., 2019)). In particular, species live in more and more fragmented habitats (Haddad et al., 2015), which reduce dispersal and partially isolate communities from one another. The metacommunity framework is key to address the responses of species and communities to perturbations in this changing world (Leibold et al., 2004; Amarasekare, 2008; Leibold and Chase, 2017). Small isolated populations are more prone to extinction (Purvis et al., 2000), and simultaneous local extinctions across sites lead to a global extinction. The asynchrony between different populations of the same species is a fundamental mechanism ensuring the global persistence and temporal stability of an entire metapopulation at the landscape scale as it reduces the risk of simultaneous extinction in all patches (Blasius et al., 1999).

While dispersal tends to synchronise populations of the same species (Abbott, 2011), dispersal of specific trophic levels can lead to synchrony or asynchrony between the various species in food chains (Koelle and Vandermeer, 2005; Pedersen et al., 2016). Species that disperse or forage across several communities can propagate trophic cascades in space, as shown empirically and theoretically (Knight et al., 2005; McCoy et al., 2009; Casini et al., 2012; García-Callejas et al., 2019); depending on which trophic levels disperse, the strength of trophic cascades within each community can be amplified or dampened (Leroux and Loreau, 2008). In addition, different food chain lengths in different sites can lead to opposite responses of different populations of the same species (Wollrab et al., 2012).

The dispersal of top predators has been particularly studied as generalist consumers linking different food webs by feeding on multiple energetic channels are ubiquitous across ecosystems (Rooney et al., 2006, 2008; Wolkovich et al., 2014; Ward et al., 2015). In particular, mobile predatory fish couple pelagic and benthic compartments in aquatic ecosystems (Vander Zanden and Vadeboncoeur, 2002; Vadeboncoeur et al., 2005), and predator dispersal leads to trophic cascades in surrounding ecosystems (Knight et al., 2005; Casini et al., 2012; Tscharntke et al., 2012). In such systems, asynchrony is promoted by the asymmetry between coupled food chains (McCann et al., 1998; Rooney et al., 2006) even when top predator populations are under correlated environmental perturbations (Vasseur and Fox, 2007).

Many of these theoretical studies have considered the synchrony of food chains that display chaotic dynamics or limit cycles (McCann et al., 1998; Koelle and Vandermeer, 2005; Rooney et al., 2006), which are characteristic of strong top-down control (Barbier and Loreau, 2019). In this case, many of the mechanisms cited above (*e.g.* top predator coupling or asymmetry) act simultaneously and interact with the variability generated internally by the limit cycles of food chain dynamics, which makes it difficult to tease apart the effects of internal and external sources of variability. perturbation propagation Variability can also be generated by stochastic external perturbations but few studies studying synchrony in metacommunities have considered these (McCann et al., 2005; Vasseur and Fox, 2007). Wang et al. (2015) used them successfully to investigate the stability of competitive metacommunities but their effects in trophic metacommunities remain poorly understood. In the context of stochastic perturbations, mechanisms such as asymmetry may not be required to get asynchrony between the different populations.

Here we propose a first step toward a more systematic approach to synchrony in trophic metacommunities near equilibrium where several species can disperse and several stochastic perturbations can affect different species independently. We aim to understand what shapes synchrony in a broad spectrum of ecological settings, dominated by either bottom-up or top-down control within a food chain (Barbier and Loreau, 2019) and by either trophic or spatial mechanisms at each trophic level. To achieve this goal, it is primordial to describe the relative contribution of perturbations and dispersal compared to the local demographic dynamics among species. In a single food chain, Barbier and Loreau (2019) showed that a few parameters control the biomass distribution among trophic levels (*i.e.* top or bottom-heavy pyramids) and the overall top-down or bottom-up behaviour of the system (*e.g.* trophic cascades). In turn, the biomass distribution drives many processes in food web dynamics. For instance, Arnoldi et al. (2019) showed that the variance generated by stochastic perturbations depends on species' biomass. Thus, perturbations with the same variance can impact the dynamics of different species more or less depending on their relative abundances.

As noted above, food web dynamics can be highly sensitive to varying dispersal rates of particular trophic levels (Koelle and Vandermeer, 2005; Pedersen et al., 2016). Comparing the absolute values of dispersal rates, however, is not meaningful when considering species with different biological rates Therefore, we rescale the dispersal rate of each species by its density-dependent mortality rate, which is assumed to be representative of various intra-specific processes, as done by Barbier and Loreau (2019) for all biological rates. More generally, quantifying the relative importance of local dynamics and dispersal processes is key to properly assess how dispersal affects the overall dynamics of each species. In fact, the relative importance of local dynamics and dispersal is what distinguishes different metacommunity paradigms (Leibold et al., 2004; Leibold and Chase, 2017); it also controls different recovery regimes after perturbations. For instance, Zelnik et al. (2019) showed that, with low dispersal and fast local dynamics, the system recovers locally from the perturbation, while with high dispersal and slow local dynamics, perturbations propagate across the whole system. In our system, we can expect the biomass distribution to affect the relative importance of local dynamics and dispersal processes as they do not scale in the same way with species biomass.

Taken together, these mechanisms must lead to situations where perturbations do not have the strongest impact on the species whose dynamics are the most impacted by dispersal. In such a situation, those perturbations can filter through the food web before being transmitted through dispersal and then affect different locations in opposite ways. A synthetic understanding of synchrony may thus be achieved by quantifying the propagation of perturbations, both vertically along food chains, and horizontally across space.

We develop a model of coupled food chains based on these recent studies and first consider a perturbation affecting a unique species in one patch and dispersal performed by a single species. Then, we explore the factors that govern synchrony between populations at the same or different trophic levels. perturbation propagation In particular, we carefully examine the effects of perturbations depending on (1) which species have the strongest response to perturbations; and (2) for which trophic level the strength of dispersal relative to demographic processes is highest. Finally, we try to disentangle the effects of several independent perturbations affecting different species. As a starting point, we consider a simple

setting with Lotka-Volterra dynamics and stochastic external perturbations around an equilibrium. This allows us to partition the variability and correlations generated by multiple perturbations. Partitioning approaches provide a powerful way to disentangle the effects of different mechanisms and to assess their relative importance (Price, 1970; Loreau and Hector, 2001; Jaillard et al., 2018). It also allows us to use simple scenarios in which a single species is perturbed as building blocks to understand more complex systems with multiple perturbations. Thus, we could assess the contribution of each species and their influence on other species to explain the synchrony or the asynchrony between the different populations.

Material and methods

The metacommunity model

We extend the model developed by Barbier and Loreau (2019). They considered a food chain model with a simple metabolic parametrisation, for which they described the biomass distribution and their responses to perturbations. Their model corresponds to the "intra-patch dynamics" part of equations (1a) and (1b) to which we graft a dispersal term to consider a metacommunity with two patches (Fig.1A).

$$\frac{dB_1}{dt} = B_1(g_1 - D_1B_1 - \alpha_{2,1}B_2) + \delta_1(B'_1 - B_1) \tag{1a}$$

$$\frac{dB_i}{dt} = \underbrace{B_i(-r_i - D_iB_i + \epsilon\alpha_{i,i-1}B_{i-1} - \alpha_{i+1,i}B_{i+1})}_{\text{Intra-patch dynamics}} + \underbrace{\delta_i(B'_i - B_i)}_{\text{Dispersal}} \tag{1b}$$

B_i is the biomass of trophic level i in the patch of interest, B'_i its biomass in the other patch, ϵ is the biomass conversion efficiency and $\alpha_{i,j}$ is the interaction strength between consumer i and prey j. Species i disperses between the two patches at rate δ_i. The density independent net growth rate of primary producers g_i in equations (1a), the mortality rate of consumers r_i in equations (1b) and the density dependent mortality rate D_i scale with species metabolic rates m_i as biological rates are linked to energy expenditure (see section S1-2 in the supporting information).

$$g_1 = m_1 g \qquad r_i = m_i r \qquad D_i = m_i D \tag{2}$$

In order to get a broad range of possible responses, we assume the predator-prey metabolic rate ratio m and the interaction strength to self-regulation ratio a to be constant. These ratios capture the relations between parameters and trophic levels. This enables us to consider contrasting situations while keeping the model as simple as possible.

$$m = \frac{m_{i+1}}{m_i} \qquad a = \frac{\alpha_{i,i-1}}{D_i} \qquad d_i = \frac{\delta_i}{D_i} \tag{3}$$

Varying m leads to food chains where predators have faster or slower biomass dynamics than their prey and varying a leads to food chains where interspecific interactions prevail or not compared with intraspecific interactions (Fig.1B). As all biological rates are rescaled by D_i, we also define d_i, the dispersal rate relative to self-regulation (referred as scaled dispersal rate in the rest of the study), in order to keep the values of the dispersal rate relative to the other biological rates consistent across trophic levels. Finally, the time scale of the system is defined by setting the metabolic rate of the primary producer m_1 to unity. Thus, we can transform equations (1a) and (1b) into:

$$\frac{1}{D}\frac{dB_1}{dt} = B_1(\frac{g}{D} - B_1 - maB_2) + d_1(B'_1 - B_1) \tag{4a}$$

$$\frac{1}{m^{i-1}D}\frac{dB_i}{dt} = \underbrace{B_i(-\frac{r}{D} - B_i + \epsilon aB_{i-1} - maB_{i+1})}_{\text{Intra-patch dynamics}} + \underbrace{d_i(B'_i - B_i)}_{\text{Dispersal}} \tag{4b}$$

Thus, ϵa and ma defines the positive effect of the prey on its predator and the negative effect of the predator on its prey, respectively (Fig.1B). These two synthetic parameters define the overall behaviour of the food chain and will be varied over the interval $[0.1, 10]$ (see Table S1-2 in the supporting information) to consider a broad range of possible responses (see Fig.2A and Barbier and Loreau (2019) for more details). Parameter values are summarised is Table S1-1 and S1-2 in the supporting information.

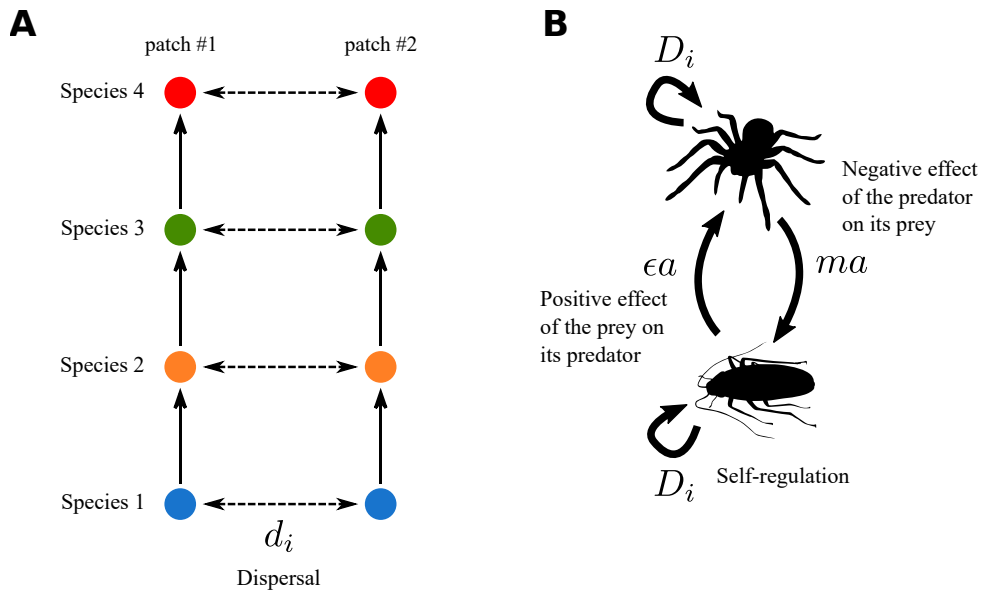

Figure 1: **A)** Metacommunity model with two patches, each containing a food chain with four trophic levels. Species disperse between the two patches at rate d_i. **B)** Predator prey model with its synthetic parameters: ϵa the positive effect of the prey on its predator, ma the negative effect of the predator on its prey and D_i the self-regulation.

Stochastic perturbations

To study the response of the metacommunity to perturbations we apply stochastic perturbations. From equations (4a) and (4b) we get the following stochastic differential equation:

$$dB_i = \underbrace{f_i(B_1, ..., B_S)dt}_{\text{Deterministic}} + \underbrace{\sigma_i B_i^z dW_i}_{\text{Perturbation}} \tag{5}$$

$f_i(B_1, ..., B_S)$ represents the deterministic part of the dynamics of species i biomass depending on the biomass of the S species present in the metacommunity (as described by equations (4a) and (4b)). Stochastic perturbations are defined by their standard deviation σ_i and dW_i, a white noise term with mean 0 and variance 1. In addition, perturbations scale with each species biomass with an exponent z. We consider two types of perturbations (Haegeman and Loreau, 2011; Arnoldi et al., 2019): demographic stochasticity (from birth-death processes) corresponds to $z = 0.5$, and environmental factors lead to $z = 1$ (see demonstration in Lande et al., 2003 and in appendix S1-3 in the supporting information). Arnoldi et al. (2019) showed that when a species is perturbed, the ratio of its biomass variance to the perturbation variance increases with the species' biomass in the case of environmental perturbations, while it is independent of its biomass in the case of demographic perturbations. Therefore, we chose demographic perturbations in our analysis as they enable us to perturb different species with the same relative intensity regardless of their abundance. This choice is made purely for modelling convenience. Although environmental perturbations may be more relevant from an ecological point of view, changing the perturbation exponent will alter only which trophic level is most affected (*e.g.* the most abundant, for environmental perturbations), not the rest of our analysis (see Fig.S2-5 in the supporting information).

Response to perturbations

We aim to determine the synchrony between populations at equilibrium when they receive small stochastic perturbations. Synchrony can be evaluated from the covariance between the temporal variations of different species and patches, which are encoded in the variance-covariance matrix C^*. Therefore, we linearise the system in the vicinity of equilibrium to get equation (6) where $X_i = B_i - B_i^*$ is the deviation from equilibrium (see section S1-4 and S1-6 in the supporting information).

$$\frac{d\vec{X}}{dt} = J\vec{X} + T\vec{E} \tag{6}$$

J is the Jacobian matrix (see section S1-5 in the supporting information) and T defines how the perturbations $E_i = \sigma_i dW_i$ apply to the system (scaling with species biomass).

Then, we get the variance-covariance matrix C^* of species biomasses (variance-covariance matrix of $\overrightarrow{X}$) from the variance-covariance matrix of perturbations V_E (variance-covariance matrix of $\overrightarrow{E}$) by solving the Lyapunov equation (7) (Arnold, 1974; Wang et al., 2015; Arnoldi et al., 2016; Shanafelt and Loreau, 2018).

$$JC^* + C^*J^\top + TV_ET^\top = 0 \tag{7}$$

The expressions of V_E and T and the method to solve the Lyapunov equation are detailed in section S1-6 in the supporting information. The variance-covariance matrix C^* can also be obtained through numerical simulations with the Euler-Maruyama method detailed in section S1-7 in the supporting information.

From the variance-covariance matrix C^* whose elements are w_{ij} we can compute the correlation matrix R^* of the system whose elements ρ_{ij} are defined by:

$$\rho_{ij} = \frac{w_{ij}}{\sqrt{w_{ii}w_{jj}}} \tag{8}$$

Processes controlling the synchrony

We first explore the general response of the food chain model to perturbations affecting specific trophic levels (or when trophic levels are perturbed). Thus, we show how the perturbations propagate vertically through the food chain depending on various ecological conditions described by the synthetic parameters summarised in figure 1B. Then, we study a simple case where only one species is perturbed and one species is able to disperse in order to identify the mechanisms leading to the asynchrony of the two populations of the same species. We finish with two more complex settings: one where all trophic levels are able to disperse at the same rate and one where all trophic levels in the two patches are affected by independent perturbations.

In the first setting, we identify the factors controlling the relative importance of demographic and dispersal processes: dispersal processes tend to correlate (or anti-correlate) populations while demographic process tend to decorrelate them. We define a metric M_1 that describes the relative weight of these two processes by taking the absolute values of the elements of equations (4a) and (4b) to assess the sheer intensity of local demographic processes and dispersal processes calculated with the equilibrium biomasses:

$$M_1 = \frac{|d_iB_i^{*'}| + |-d_iB_i^*|}{|\epsilon aB_{i-1}^*B_i^*| + |d_iB_i^{*'}| + |-\frac{r}{D}B_i^*| + |-B_i^{*2}| + |-maB_{i+1}^*B_i^*| + |-d_iB_i^*|} \tag{9}$$

In the second setting, we use the Lyapunov equation to partition the effect of each perturbation and to disentangle the contribution of each perturbation and each trophic level to the correlation pattern.

Results

General responses of the food chain model to perturbations

We first describe the biomass distribution and the responses to perturbations of an isolated food chain (*i.e.* without considering spacial dynamics). We use a broad range of physiological and ecological parameters to describe all the possible responses of the food chain model (Fig.2A). ma represents the strength of negative interactions (mortality due to predation) while ϵa represents the strength of positive interactions (biomass gain due to consumption)(Fig.1B). As in Barbier and Loreau (2019), the food chain displays various biomass distributions in different regimes: bottom-heavy (for $\epsilon a = 0.1$) biomass pyramids, top-heavy biomass pyramids (for $\epsilon a = 10$ and $ma = 0.1$) or alternating "cascade" patterns (for $\epsilon a = 10$ and $ma = 10$).

In each case, we can capture the dynamical behaviour of the food chain by considering the correlation matrix of the response of each species to perturbations applied to specific trophic levels (Fig.2B). Perturbing primary producers leads to bottom-up responses in which adjacent trophic levels are correlated, *i.e.* their biomasses respond in the same way, (Fig.2B and 2C) while perturbing top predators leads to top-down responses in which adjacent trophic levels are anti-correlated, *i.e.* their biomasses respond in opposite ways, (Fig.2B and 2D).

When all species receive independent stochastic demographic perturbations (Fig.S2-1A in the supporting information), the correlation pattern is dominated by bottom-up effects for high values of ma ($ma = 10$, which corresponds to the strongest responses in Fig.2C) and is top-down for low values of ma ($ma \leq 1$, which corresponds to the strongest responses in Fig.2D, see also Fig.S2-1C in the supporting information).

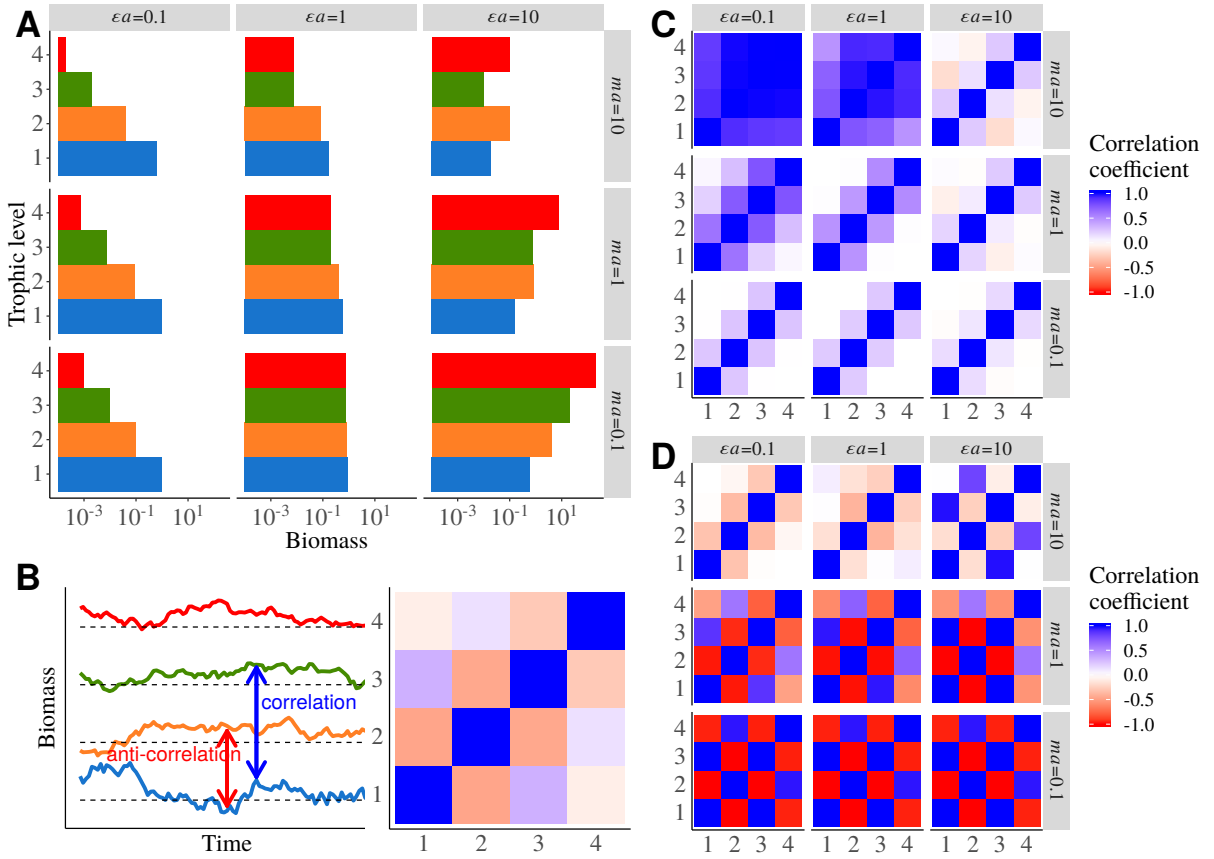

Figure 2: General description of an isolated food chain ($d_i = 0$, no dispersal) for nine combinations of the physiological and ecological parameters ϵa and ma that respectively describe the positive effect of biomass consumption and the negative effects mortality due to predation (see Barbier and Loreau (2019)). **A)** Biomass distribution among trophic levels. **B)** Correlation between species biomass dynamics. The correlations seen in time series are represented by a correlation matrix where each element is the correlation coefficient between two species. Thus, the matrix is symmetric and the diagonal elements are equal to 1 as each species is perfectly autocorrelated. **C)** Correlation matrix within a food chain with a demographic stochastic perturbation applied to primary producers. **D)** Same correlation matrix with a demographic stochastic perturbation applied to top predators.

Propagation of a perturbation when one species disperses

Perturbations can propagate vertically within a food chain or horizontally between food chains. To understand how these two types of propagations shape the synchrony between patches we first consider a simple case where only primary producers are perturbed in patch #1 (patch #2 being the unperturbed patch) and only top predators disperse (Fig.3A).

In patch #1, the perturbation has a bottom-up effect that correlates species (Fig.3B, label (1)) as in Fig.2C where primary producers are also directly perturbed. While in patch #2, the perturbation has a top-down transmission (Fig.3A), leading to an anti-correlation of adjacent trophic levels (Fig.3B, label (2)), which is similar to Fig.2D as the transmission of the perturbation by top predators is equivalent to a direct perturbations of top predators in patch #2. Then, the different correlation patterns within each patch affect the synchrony between the two patches. First, the two populations of top predators are perfectly correlated as they are directly coupled through dispersal (Fig.3B, label (3)). Second, the populations of carnivores are anti-correlated because they are respectively correlated and anti-correlated to top predators in patch #1 and #2 (Fig.3B, (4)). Similarly, the correlation between each trophic level and top predators in each patch drives the correlation between the two population at lower trophic levels.

For whom does dispersal matter?

Now, all species disperse at the same rate d_i but we still consider perturbations only affecting the primary producers in patch #1. Even if all scaled dispersal rates are equal, the relative importance of dispersal processes compared to intra-patch demography quantified by M_1 (see equation (9)) differs between species. When scaled dispersal rates d_i increase, M_1 first increases for top predators, then for

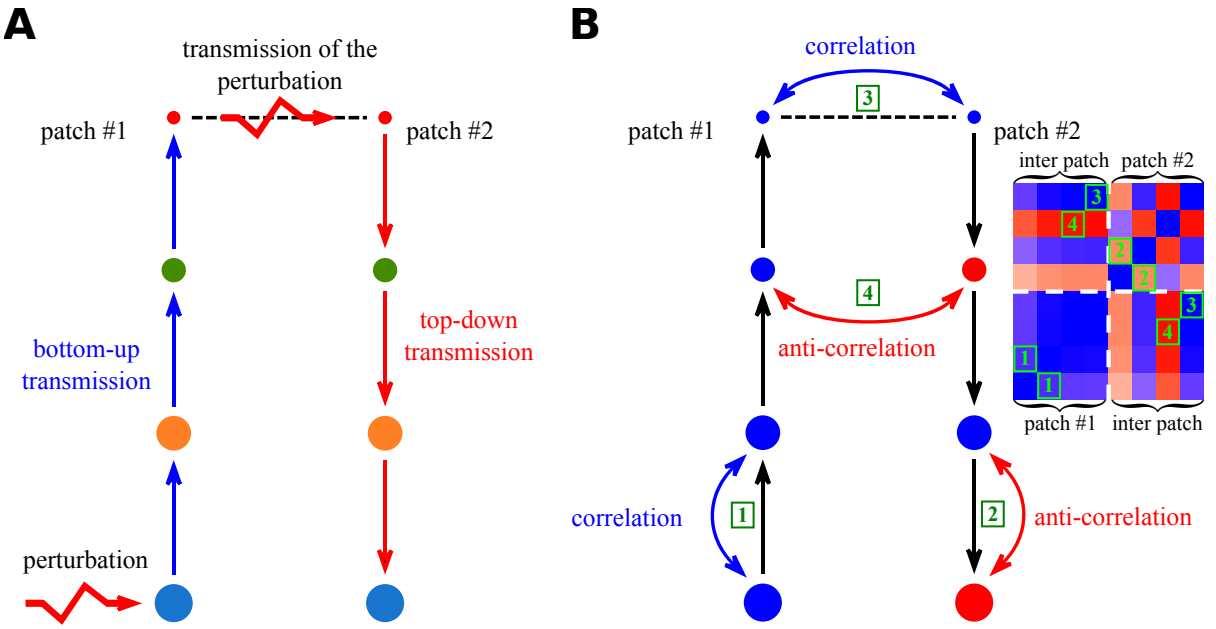

Figure 3: Transmission of perturbations between the two patches (primary producers perturbed in patch #1, $\epsilon a = 0.1$, $ma = 10$ and only top predators disperse). Disk size represents species abundance. **A)** Only top predators are able to disperse, transmitting the perturbation between patches. They convert the bottom-up perturbation from patch #1 into a top-down perturbation in patch #2. **B)** The bottom-up transmission in patch #1 leads to correlations between adjacent trophic levels (label 1) while the top-down transmission leads to anti-correlations between adjacent trophic levels in patch #2 (2). Dispersal directly couples the two populations of top predators that act as one unique population, thus, they are completely correlated (3). The different correlation patterns within each patch lead to correlations or anti-correlations between populations of the same species in different patches depending on its distance from top predators (4).

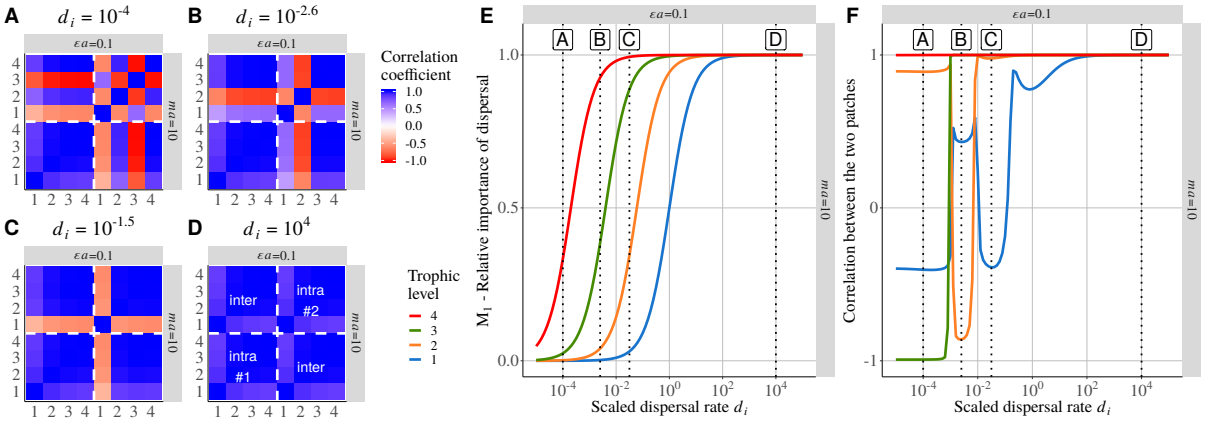

Figure 4: Correlation between populations of four species forming a food chain present in two connected patches ($\epsilon a = 0.1$, $ma = 10$). Primary producers in patch #1 receive demographic perturbations while patch #2 is not directly perturbed. **A)**, **B)**, **C)** and **D)** are correlation matrices between species within and between patches for four different scaled dispersal rates d_i. Diagonal blocks represent intra-patch species correlations while the other blocks represent inter-patch species correlations (see the labels in **D)**). The bottom-left block represents the perturbed patch (#1) while the top-right block represents the unperturbed patch (#2) (see Fig.3B). **E)** M_1, ratio of dispersal processes to the sum demographic and dispersal processes (see equation (9)) for each trophic level with increasing scaled dispersal rates. Labels A, B, C and D respectively refer to the values of scaled dispersal rates used to plot the correlation matrices presented in **A)**, **B)**, **C)** and **D)**. **F)** Correlation between populations of the same species from two patches for increasing scaled dispersal rates d_i (equal for all species). The represented correlations are equal to the diagonal elements of the off-diagonal blocks of correlation matrix (inter).

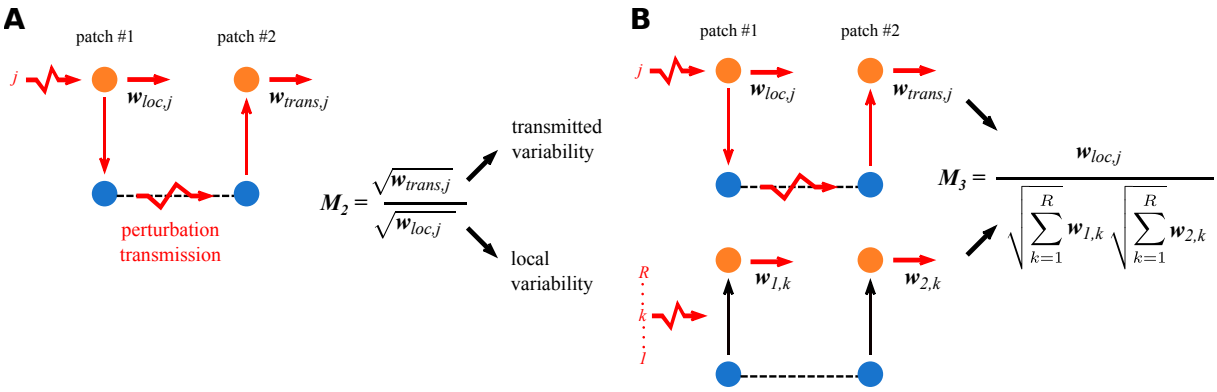

Figure 5: Metrics weighting the contribution of each perturbation to the correlation pattern generated by multiple perturbations. $w_{1,j}$ and $w_{2,j}$, which are element of the matrix $C^*_{S,j}$, are the variance of species i in patches #1 and #2 respectively when perturbation j is applied. We define $w_{loc,j}$ the variability directly generated by the perturbation and $w_{trans,j}$ the variability transmitted in the other patch. $w_{loc,j}$ and $w_{trans,j}$ are respectively equal to $w_{1,j}$ (or $w_{2,j}$) and $w_{2,j}$ (or $w_{1,j}$) when perturbation j is applied in patch #1 (or #2). **A)** M_{2_j} is the ratio of transmitted variability $w_{trans,j}$ to local variability $w_{loc,j}$. **B)** M_{3_j} weights the effect of each perturbation j by the variability it generates locally compared to the other perturbations.

carnivores and so on until primary producers (Fig.4E). This is due to biomass distribution (Fig.2A) as dispersal scales linearly with biomass while intra-patch demography scales with squared biomass (self-regulation) or biomass products (predation) (see equations (4a) and (4b) and Fig.S2-1E in the supporting information).

At low scaled dispersal rates (*e.g.* $d_i = 10^{-4}$), dispersal matters only for top predators (Fig.4E label A), leading to a situation already described by Fig.3. At intermediate scaled dispersal rates (*e.g.* $d_i = 10^{-2.6}$), dispersal also matters for carnivores (Fig.4E label B). Thus, top predators and carnivores are correlated between patches and we observe anti-correlations between adjacent trophic levels lower than 4 (Fig.4B). This time, this leads to the anti-correlation of sub-populations of herbivores (Fig.4F label B) while they were correlated previously (Fig.3B and Fig.4F label A). Therefore, each time dispersal starts to matter for another trophic level, the correlation pattern in patch #2 changes (Fig.4A-D), leading to shifts between correlations and anti-correlations between the populations of lower trophic levels (Fig.4F).

Multiple perturbation partitioning

The case displayed in Fig.4 was easy to handle as only one perturbation was applied and we knew for which species dispersal mattered. Such a simple case can actually act as a building block to understand correlation patterns produced by multiple perturbations. In fact, for R independent perturbations, the variance-covariance matrix C^*_S is equal to the sum of the variance-covariance matrices $C^*_{S,j}$ obtained when only one perturbation j is applied, $C^*_S = \sum_{j=1}^{R} C^*_{S,j}$ (see section S2-3-1 in the supporting information). Then, correlations between the populations of species i can be expressed as the sum of the correlations obtained when each perturbation j is applied alone weighted by the corresponding variance in the two patches.

$$\rho_i = \sum_{j=1}^{R} \rho_{i,j} M_{2_j} M_{3_j} \tag{10}$$

R is the number of independent perturbations, ρ_i is the correlation coefficient between the two populations of species i and $\rho_{i,j}$ is the same correlation coefficient in the case where only perturbation j is applied. M_{2_j} quantifies the variability generated locally by perturbation j that is effectively transmitted to the other patch (Fig.5A). If M_{2_j} is close to zero, the perturbation is poorly transmitted and the two patches will probably be asynchronous. M_{3_j} weights each $\rho_{i,j}$ by the variability generated by perturbation j compared to the other perturbations (Fig.5B). If M_{3_j} is low, perturbation j would generate less variability than the other perturbations and the associated correlation $\rho_{i,j}$ will not significantly contribute to the correlation ρ_i generated by all perturbations.

In the following, we present a simple case with two species in each patch receiving independent demographic stochastic perturbations and only primary producers are able to disperse (see Fig.S2-3 in the supporting information for an example with four species). In Fig.6, we illustrate step by step the decomposition of the correlation pattern generated by multiple perturbations (Fig.6G).

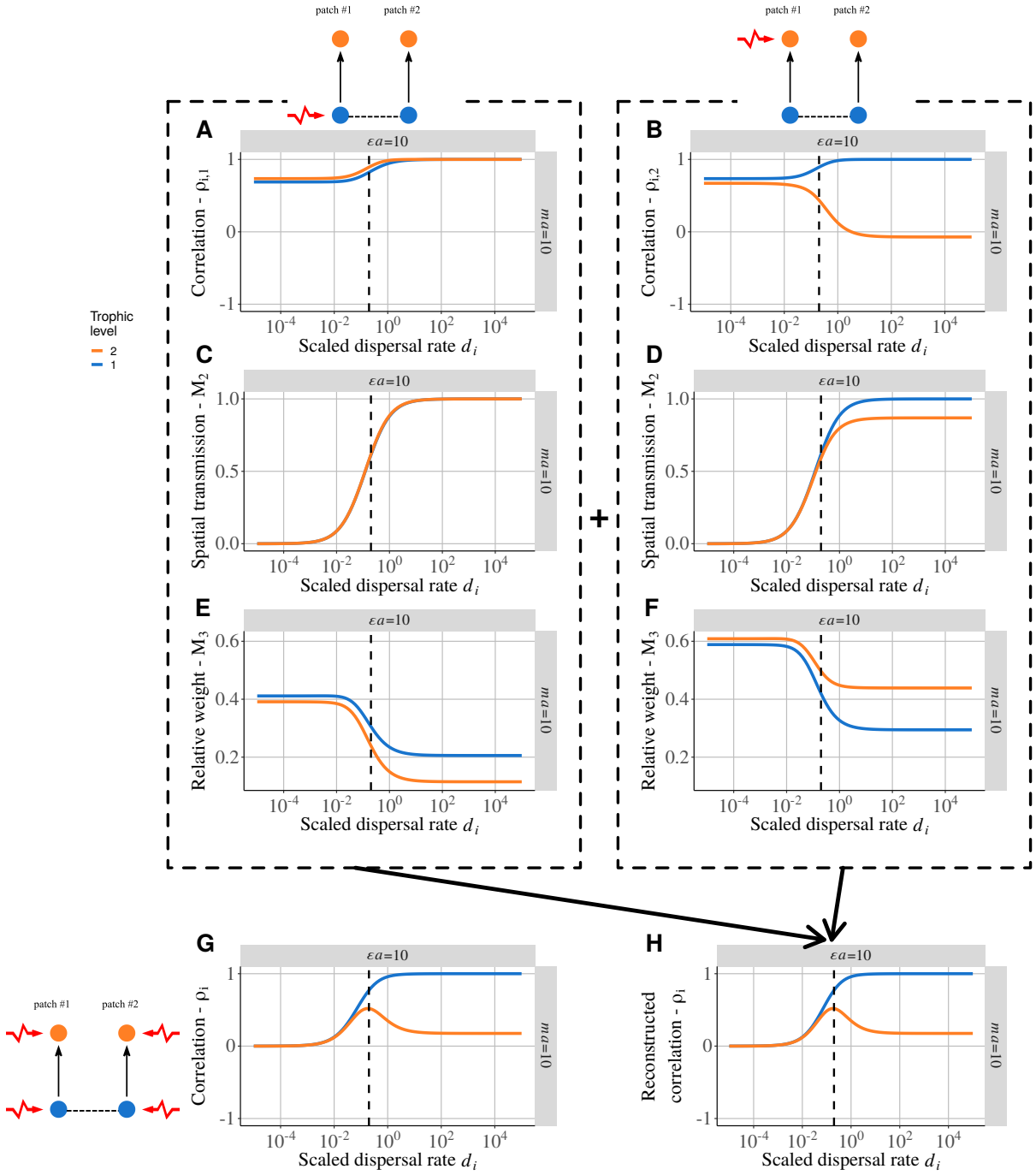

Figure 6: Detailed correlation pattern between two coupled primary producer-herbivore food chains for $\epsilon a = 10$ and $ma = 10$ with increasing scaled dispersal rates d_i. Only primary producers are able to disperse. **A)** Correlation between patches when only primary producers and **B)** herbivores from patch #1 are perturbed. **C)** Relative importance of transmitted variability to local variability (M_2) when primary producers and **D)** when herbivores are perturbed in patch #1. **E)** Relative weight of the variance generated by each perturbation (M_3) when primary producers and **F)** when herbivores are perturbed in patch #1. **G)** Correlation between patches when independent demographic stochastic perturbations are applied to all species of each patch. **H)** Reconstructed correlation pattern obtained thanks to equation (10). **H**=2(**A**×**C**×**E**+**B**×**D**×**F**) by symmetry as both patch #1 and #2 receive similar independent perturbations.

When only primary producers are perturbed in patch #1, both primary producers and herbivores are correlated due to the bottom-up transmission of the perturbation in both patches as only primary producers disperse (Fig.6A). However, when only herbivores are perturbed, herbivores become decorrelated as scaled dispersal rates d_i increase (Fig.6B) due to the weak correlation between adjacent trophic levels for $\epsilon a = 10$ and $ma = 10$ (see Fig.2C and 2D).

Our metric M_2 is equal to zero at low scaled dispersal rates d_i (Fig.6C and 6D), thus indicating that the perturbations in patch #1 are weakly transmitted in patch #2. At high scaled dispersal rates d_i, M_2 tends to 1 as species become perfectly correlated except for herbivores in Fig.6D. In this case, as they are perturbed but do not disperse, the perturbation is attenuated during its transmission through primary producers.

In this example, our metric M_3 is higher for both primary producers and herbivores when the perturbation is applied to herbivores (Fig.6F) than to primary producers (Fig.6E). This means that perturbations applied to herbivores generate most of the variability in the metacommunity and the correlation pattern in Fig.6B thus strongly contributes to the reconstructed correlation pattern gathering the effects of all perturbations (Fig.6H) following equation (10).

Now we have the response of all the elements of equation (10), we can explain the correlation pattern seen in Fig.6H. At low scaled dispersal rates d_i, perturbations are not transmitted ($M_2 = 0$), letting the two patch independent and uncorrelated, while at high scaled dispersal rates d_i, the correlation pattern is similar to Fig.6B as herbivore perturbation generates most of the variability. In between, we have a humped-shaped relationship between herbivore population correlation and scaled dispersal rates d_i because when perturbations start to be transmitted (Fig.6C and 6D), herbivore populations are correlated (left to the dashed line) (Fig.6A and 6B). Then, the decrease in Fig.6B leads to the decrease seen in Fig.6H.

The reconstructed correlation pattern in Fig.6H is identical to the correlation pattern obtained by perturbing directly each species in each patch (Fig.6G), thus demonstrating the validity of equation (10) (see Fig.S2-4 in the supporting information).

Discussion

Our metacommunity model aimed to understand how perturbations propagates vertically in patches and horizontally between patches to identify under which conditions species responses in different patches can be synchronous or asynchronous. First, we found that less abundant species are more affected by dispersal. Thus, even when all species disperse at the same scaled rate, the biomass distribution in a food chain determines for which species dispersal contributes most to biomass dynamics. In addition, if the perturbed species does not disperse enough to synchronise its different populations, the perturbation can be transmitted by other species. In such a situation, we found that species responses in different patches can be asynchronous. Second, we found that the effects of multiple independent perturbations can be partitioned. This enabled us to use simple situations in which a single species is perturbed as building blocks to analyse more complex systems with multiple perturbations. Thus, we were able to identify which perturbations drove synchrony or asynchrony in this context and thus to explain their contribution using two simple metrics.

For whom does dispersal matter?

Knowing who disperses is crucial to understand biomass dynamics in metacommunities (Koelle and Vandermeer, 2005; Pedersen et al., 2016). However, even when dispersal is homogeneous among the various species (*i.e.* same scaled dispersal rates d_i for all species), increasing dispersal does not affect all species in the same way (Fig.7). In fact, abundant species are more affected by demographic processes such as self-regulation, which scales as the square of biomass, or trophic interactions, which scale as the product of predator and prey biomass (see equation (9)). Thus, changes in scaled dispersal rates lead to top-down or bottom-up coupling between patches depending on biomass distribution.

Once we know for whom dispersal matters, the model can be simplified to a metacommunity where only a few species connect patches. With such a restricted dispersal, perturbing a species in one patch can lead to an opposite response in the other connected patch. In fact, perturbations affecting basal species have a bottom-up propagation (Fig.2C) and correlate all the species from the same food chain, while perturbations affecting top species have a top-down propagation and create trophic cascade correlation patterns (Fig.2D). Thus, if the perturbed species are not the dispersing species, both patches can display different correlation patterns, which can lead to anti-correlated responses of the different populations of the same species and hence to asynchrony between the different populations (Fig.S2-1E, Fig.S2-2A and S2-2B in supporting information). The correlation or anti-correlation of populations depends on the

shortest trophic distance from the dispersing species, as suggested by Wollrab et al. (2012). Species at odd distance have correlated population fluctuations, while species at even distance have anti-correlated population fluctuations (Fig.3A).

The case where bottom-up perturbations are transmitted by top predators is related to the spillover process: a predator population thrives due to resource abundance in one patch and spills over to the other patches (Holt, 1984). For instance, favourable environmental conditions in the Baltic main basin increase cod abundance (bottom-up control) that colonise the Gulf of Riga, leading to a trophic cascade in this locality (top-down response) (Casini et al., 2012). More generally, predators cast a "shadow" that leads to trophic cascades around their source patch (McCoy et al., 2009). For instance, dragonflies that prey on flying insects around ponds reduce pollination there (Knight et al., 2005). Such dynamics of predators between natural habitats and crop fields are central in pest biocontrol (Tscharntke et al., 2012).

The bottom-up coupling between patches does not seem to be mediated by primary producers, which often have a low mobility (sessile terrestrial plants or drifting phytoplankton), but rather by non-living materials (Polis et al., 1997; Leroux and Loreau, 2008). Marleau et al., 2010 and Gounand et al., 2014 found in their models with limit cycles that flows of nutrients lead to anti-correlations between species populations, while we found a succession of correlations and anti-correlations. This suggests that systems with limit cycles respond differently to bottom-up coupling than systems in the vicinity of an equilibrium that receive stochastic perturbations because of processes such as phase-locking (Jansen, 1999; Liebhold et al., 2004; Vasseur and Fox, 2009). Abiotic resources can link very different food webs. For instance, mineral nutrients and dead organic matter link green and brown food webs (Wolkovich et al., 2014; Buchkowski et al., 2019) but additional mechanisms such as different food chain length, omnivory or stoichiometric constraints (Attayde and Ripa, 2008; Zou et al., 2016) make a direct comparison difficult. Nevertheless, our model gives basic insights into how a simple bottom-up coupling affects the dynamics of connected food chains and should improve our understanding of the additional effects brought by mechanisms such as different food chain length or stoichiometric constraints.

While top predator dispersal or basal resource diffusion have been extensively studied, the consequences of intermediate trophic level dispersal remain poorly understood. Our results show that the dispersal of intermediate trophic levels can dramatically change the correlation between populations of non-dispersing species. Pedersen et al., 2016 found that herbivores with a lower dispersal rate than primary producers or carnivores stabilise metacommunity dynamics (by having equilibria or asynchronous limit cycles).

Most of the studies on coupled food webs considered systems displaying limit-cycles (McCann et al., 1998; Post et al., 2000; Koelle and Vandermeer, 2005) and largely ignored stochastic perturbations (McCann et al., 2005; Vasseur and Fox, 2007). Our results suggest that dispersal patterns that leads to more asynchrony depend on which species is perturbed. If the most perturbed species is also the most affected by dispersal, it transmits the perturbation to all patches and synchronise them, thus reducing the stability of the system. Otherwise, asynchrony between patches can be promoted. Thus, the stabilising or destabilising effect of dispersal patterns is not absolute and depends on perturbations.

In addition, perturbations can target specific species (*e.g.* harvesting, disease...) or affect all the species in different ways. For instance, Arnoldi et al., 2019 showed that environmental perturbations ($z = 1$) mostly affect abundant species (Fig.7 and see Fig.S2-1B, S2-2D and S2-5 in the supporting information). Therefore, considering the biomass distribution is critical to fully understand the responses of coupled food chains to dispersal and perturbations.

Multiple perturbation partitioning

Complex correlation patterns produced by multiple independent perturbations on different species in different patches can be easily partitioned into a sum of correlation patterns produced by a single perturbation (Fig.7). Such a partitioning is permitted by two characteristics of our model. First, the system is linearised. Thus, the temporal variations of each species in the vicinity of the equilibrium are the sum of the variations due to each interacting species. Second, the partitioning of the correlation pattern is permitted by the independence of the various perturbations. In fact, we can decompose the variance-covariance matrix of perturbation V_E into a sum of matrices V_{Ej} corresponding to the perturbation of a single species in a single patch (see equation (31) in section S2-3-1 in the supporting information). If some perturbations are correlated, we can still decompose the matrix V_E into a sum of independent blocks of correlated perturbations. The contribution of each perturbation in an assemblage of many independent perturbations can thus be easily understood as the product of the correlations between populations from the two patches is weighted by the variability generated in each patch (Fig.7).

Such a detailed partition of the contribution of each element of the system is not possible in systems displaying non-linear dynamics. For instance, Koelle and Vandermeer (2005) tested the effects of primary

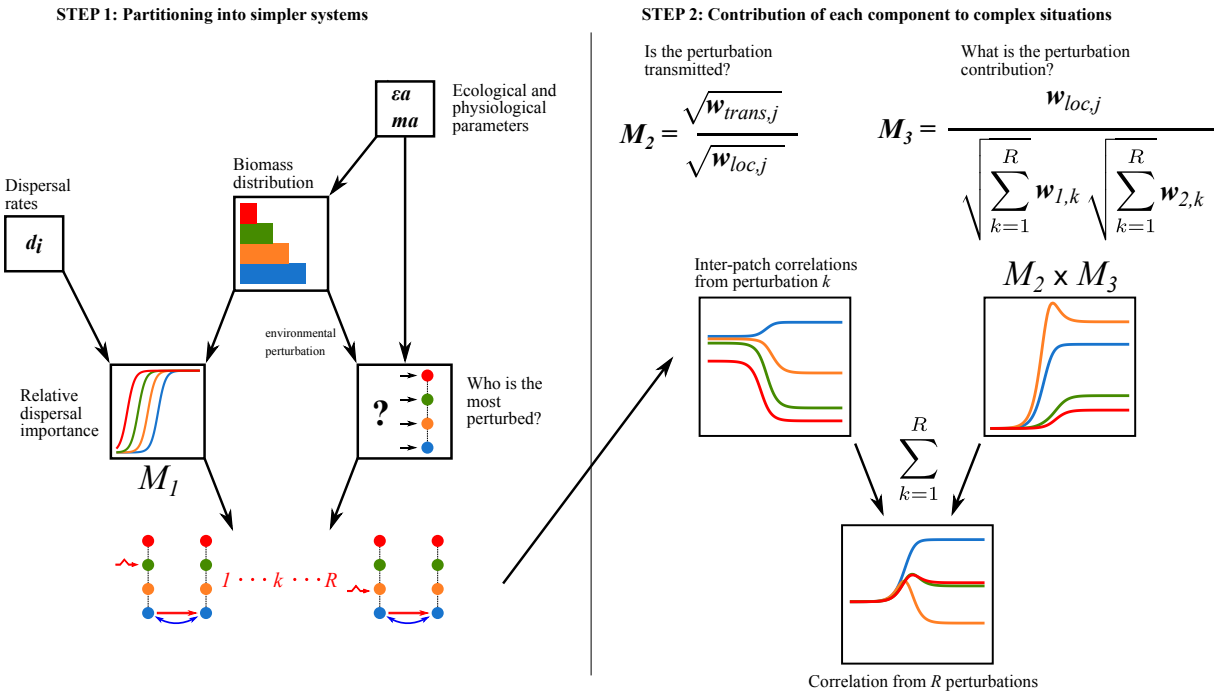

Figure 7: Sequential framework to understand the transmission of perturbations in metacommunities. Biomass distribution (driven by physiological and ecological parameters) is central as less abundant species are more affected by dispersal (metric M_1) and are less affected by environmental perturbations. Knowing that, we can simplify the system into a metacommunity where only a few species disperse and are perturbed. The effects of each perturbations can then be partitioned to understand how much they contribute to the total correlation between patches. The contribution of each perturbation can be interpreted by two metrics: M_2 that quantifies how much of the generated variability is transmitted through dispersal and M_3 that quantifies the how much variability is generated compared to other perturbations. Therefore, $M_2 \times M_3$ weights the correlation generated by each perturbation to reconstruct the correlation pattern obtained when multiple perturbations are applied.

producer and top predator dispersal on population synchrony. They found that these two types of dispersal led to either asynchrony or synchrony between the populations of the other trophic levels but they were unable to go deeper in their interpretation. Their results are similar to our case where a perturbation is applied to top predators only and primary producers disperse (Fig.S2-2B). Thus, the top predator-prey interaction must generate most of the variability in their system with limit cycles and may be equivalent to a perturbation of top predators in our linear system. Therefore, our model with linear dynamics could give clues to understand the response of models with non-linear dynamics. Future investigations considering stochastic perturbations in models with type II functional responses are required to go deeper in the comparison between systems with linear or non-linear dynamics.

Independence between perturbations is also a key feature of our study as we explained earlier. Correlations between perturbations is expected to change the observed dynamics (Ripa and Ives, 2003; Vasseur and Fox, 2007). Leroux and Loreau, 2012 considered reciprocal pulsed subsidies within a metacommunity model and demonstrated that the time delay between perturbations in each patch could reinforce or dampen the resulting oscillations. This suggests that the correlation pattern observed in our model when species from both patches are perturbed should be modified if perturbations are more or less correlated.

Conclusion

Our model demonstrates that asynchrony between populations in trophic metacommunities is promoted when the species the most affected by dispersal is not directly perturbed. The effect of dispersal on biomass dynamics compared to local demographic processes depends on the biomass distribution in food chains even if all species disperse at the same scaled rate. Thus, our simple model can serve as a good null model to test mechanisms involved in dispersal. Our model must be considered as a null model in general as it relies on strong assumptions (*e.g.* m constant across the food chain) to build a simple model to derive broad conclusions (Barbier and Loreau, 2019). The results of future studies considering more realistic situations will surely deviate from our model, but our conclusions should still be useful as

each predator-prey couple will correspond to one set of parameters used in our figures.

Dispersal can be seen as a mechanism of optimal foraging where predators follow their prey in the patch where they are the most abundant. Dispersal also enables prey to escape their predators by migrating in a "refuge" patch where they are less abundant. This can be represented by density-dependent dispersal rates, which have a strong impact on dynamics (Hauzy et al., 2010; Liu et al., 2016). However, density-dependent dispersal changes the relative importance of dispersal and local demography as dispersal then scales with biomass similarly to self-regulation or predation, thus changing the interplay between dispersal and biomass distribution. Therefore, future studies should consider biomass distribution among species to properly assess the effects of dispersal on food chain dynamics.

When multiple perturbations are applied, the effects of each perturbation and each species can be partitioned in our model. Thus, future studies considering heterogeneity between patches would be able to isolate the contribution of the difference of parameters to food chain dynamics. For instance, Rooney et al. (2006) considered two food chains with different attack rates and coupled by a mobile top predator. In this case, perturbation partitioning would enable us to deeply understand how such differences between food chains may dampen perturbation transmission or promote asynchrony.

Thus, our approach appears to be a promising tool to better understand the effects of many mechanisms that promote stability or asynchrony in coupled food chains or trophic metacommunities.

Acknowledgement

We thank Charlotte T. Lee and the two anonymous reviewers for their constructive comments. This work was supported by the TULIP Laboratory of Excellence (ANR-10-LABX-41) and by the BIOSTASES Advanced Grant, funded by the European Research Council under the European Union's Horizon 2020 research and innovation programme (666971).

Author contribution

Conceptualisation (PQ, MB, ML) - Funding acquisition (ML) - Model analysis (PQ, MB, ML) - Coding simulation (PQ) - Supervision (ML) - Original draft writing (PQ) - Review & editing (MB, ML)

Data accessibility

The C++ code of the simulations and the R code of the figures are available on Zenodo (doi: 10.5281/zenodo.3613500). doi:10.5281/zenodo.3613500

References

Abbott, K. C. (2011). A dispersal-induced paradox: Synchrony and stability in stochastic metapopulations. *Ecology Letters*, *14*(11), 1158–1169. doi:10.1111/j.1461-0248.2011.01670.x

Amarasekare, P. (2008). Spatial dynamics of foodwebs. *Annual Review of Ecology, Evolution, and Systematics*, *39*(1), 479–500. doi:10.1146/annurev.ecolsys.39.110707.173434

Arnold, L. (1974). *Stochastic differential equations: Theory and applications*. New York: Wiley.

Arnoldi, J., Loreau, M., & Haegeman, B. (2016). Resilience, reactivity and variability: A mathematical comparison of ecological stability measures. *Journal of Theoretical Biology*, *389*, 47–59. doi:10.1016/j.jtbi.2015.10.012

Arnoldi, J., Loreau, M., & Haegeman, B. (2019). The inherent multidimensionality of temporal variability: How common and rare species shape stability patterns. *Ecology Letters*, *22*(10), 1557–1567. doi:10.1111/ele.13345

Attayde, J. L. & Ripa, J. (2008). The coupling between grazing and detritus food chains and the strength of trophic cascades across a gradient of nutrient enrichment. *Ecosystems*, *11*(6), 980–990. doi:10.1007/s10021-008-9174-8

Barbier, M. & Loreau, M. (2019). Pyramids and cascades: A synthesis of food chain functioning and stability. *Ecology Letters*, *22*(2), 405–419. doi:10.1111/ele.13196

Blasius, B., Huppert, A., & Stone, L. (1999). Complex dynamics and phase synchronization in spatially extended ecological systems. *Nature*, *399*(6734), 354–359. doi:10.1038/20676

Buchkowski, R. W., Schmitz, O. J., & Bradford, M. A. (2019). Nitrogen recycling in coupled green and brown food webs: Weak effects of herbivory and detritivory when nitrogen passes through soil. *Journal of Ecology*, *107*(2), 963–976. doi:10.1111/1365-2745.13079

Casini, M., Blenckner, T., Mollmann, C., Gardmark, A., Lindegren, M., Llope, M., ... Stenseth, N. C. (2012). Predator transitory spillover induces trophic cascades in ecological sinks. *Proceedings of the National Academy of Sciences*, *109*(21), 8185–8189. doi:10.1073/pnas.1113286109

Díaz, S., Settele, J., Brondizio, E., Ngo, H. T., Guèze, M., Agard, J., ... Zayas, C. (2019). *Summary for policymakers of the global assessment report on biodiversity and ecosystem services of the Intergovernmental Science-Policy Platform on Biodiversity and Ecosystem Services*. Bonn, Germany: IPBES.

García-Callejas, D., Molowny-Horas, R., Araújo, M. B., & Gravel, D. (2019). Spatial trophic cascades in communities connected by dispersal and foraging. *Ecology*, *100*(11). doi:10.1002/ecy.2820

Gounand, I., Mouquet, N., Canard, E., Guichard, F., Hauzy, C., & Gravel, D. (2014). The paradox of enrichment in metaecosystems. *The American Naturalist*, *184*(6), 752–763. doi:10.1086/678406

Haddad, N. M., Brudvig, L. A., Clobert, J., Davies, K. F., Gonzalez, A., Holt, R. D., ... Townshend, J. R. (2015). Habitat fragmentation and its lasting impact on Earth's ecosystems. *Science Advances*, *1*(2), e1500052. doi:10.1126/sciadv.1500052

Haegeman, B. & Loreau, M. (2011). A mathematical synthesis of niche and neutral theories in community ecology. *Journal of Theoretical Biology*, *269*(1), 150–165. doi:10.1016/j.jtbi.2010.10.006

Hauzy, C., Gauduchon, M., Hulot, F. D., & Loreau, M. (2010). Density-dependent dispersal and relative dispersal affect the stability of predator–prey metacommunities. *Journal of Theoretical Biology*, *266*(3), 458–469. doi:10.1016/j.jtbi.2010.07.008

Holt, R. D. (1984). Spatial heterogeneity, indirect interactions, and the coexistence of prey species. *The American Naturalist*, *124*(3), 377–406. doi:10.1086/284280

Jaillard, B., Richon, C., Deleporte, P., Loreau, M., & Violle, C. (2018). An a posteriori species clustering for quantifying the effects of species interactions on ecosystem functioning. *Methods in Ecology and Evolution*, *9*(3), 704–715. doi:10.1111/2041-210X.12920

Jansen, V. A. A. (1999). Phase locking: Another cause of synchronicity in predator–prey systems. *Trends in Ecology & Evolution*, *14*(7), 278–279. doi:10.1016/S0169-5347(99)01654-7

Knight, T. M., McCoy, M. W., Chase, J. M., McCoy, K. A., & Holt, R. D. (2005). Trophic cascades across ecosystems. *Nature*, *437*(7060), 880–883. doi:10.1038/nature03962

Koelle, K. & Vandermeer, J. (2005). Dispersal-induced desynchronization: From metapopulations to metacommunities. *Ecology Letters*, *8*(2), 167–175. doi:10.1111/j.1461-0248.2004.00703.x

Lande, R., Engen, S., & Saether, B.-E. (2003). *Stochastic population dynamics in ecology and conservation*. Oxford University Press. doi:10.1093/acprof:oso/9780198525257.001.0001

Leibold, M. A. & Chase, J. M. (2017). *Metacommunity Ecology, Volume 59*. Princeton University Press. doi:10.2307/j.ctt1wf4d24

Leibold, M. A., Holyoak, M., Mouquet, N., Amarasekare, P., Chase, J. M., Hoopes, M. F., ... Gonzalez, A. (2004). The metacommunity concept: A framework for multi-scale community ecology. *Ecology Letters*, *7*(7), 601–613. doi:10.1111/j.1461-0248.2004.00608.x

Leroux, S. J. & Loreau, M. (2008). Subsidy hypothesis and strength of trophic cascades across ecosystems. *Ecology Letters*, *11*(11), 1147–1156. doi:10.1111/j.1461-0248.2008.01235.x

Leroux, S. J. & Loreau, M. (2012). Dynamics of reciprocal pulsed subsidies in local and meta-ecosystems. *Ecosystems*, *15*(1), 48–59. doi:10.1007/s10021-011-9492-0

Liebhold, A., Koenig, W. D., & Bjørnstad, O. N. (2004). Spatial synchrony in population dynamics. *Annual Review of Ecology, Evolution, and Systematics*, *35*(1), 467–490. doi:10.1146/annurev.ecolsys.34.011802.132516

Liu, Z., Zhang, F., & Hui, C. (2016). Density-dependent dispersal complicates spatial synchrony in tritrophic food chains. *Population Ecology*, *58*(1), 223–230. doi:10.1007/s10144-015-0515-0

Loreau, M. & Hector, A. (2001). Partitioning selection and complementarity in biodiversity experiments. *Nature*, *412*(6842), 72–76. doi:10.1038/35083573

Marleau, J. N., Guichard, F., Mallard, F., & Loreau, M. (2010). Nutrient flows between ecosystems can destabilize simple food chains. *Journal of Theoretical Biology*, *266*(1), 162–174. doi:10.1016/j.jtbi.2010.06.022

McCann, K. S., Hastings, A., & Huxel, G. R. (1998). Weak trophic interactions and the balance of nature. *Nature*, *395*(6704), 794–798. doi:10.1038/27427

McCann, K. S., Rasmussen, J. B., & Umbanhowar, J. (2005). The dynamics of spatially coupled food webs. *Ecology Letters*, *8*(5), 513–523. doi:10.1111/j.1461-0248.2005.00742.x

McCoy, M. W., Barfield, M., & Holt, R. D. (2009). Predator shadows: Complex life histories as generators of spatially patterned indirect interactions across ecosystems. *Oikos*, *118*(1), 87–100. doi:10.1111/j.1600-0706.2008.16878.x

Pedersen, E. J., Marleau, J. N., Granados, M., Moeller, H. V., & Guichard, F. (2016). Nonhierarchical dispersal promotes stability and resilience in a tritrophic metacommunity. *The American Naturalist*, *187*(5), E116–E128. doi:10.1086/685773

Polis, G. A., Anderson, W. B., & Holt, R. D. (1997). Toward an integration of landscape and food web ecology: The dynamics of spatially subsidized food webs. *Annual Review of Ecology and Systematics*, *28*, 289–316. Retrieved December 22, 2017, from http://www.jstor.org/stable/2952495

Post, D. M., Conners, M. E., & Goldberg, D. S. (2000). Prey preference by a top-predator and the stability of linked food chains. *Ecology*, *81*(1), 8–14. doi:10.1890/0012-9658(2000)081[0008:PPBATP]2.0.CO;2

Price, G. R. (1970). Selection and covariance. *Nature*, *227*(5257), 520–521. doi:10.1038/227520a0

Purvis, A., Gittleman, J. L., Cowlishaw, G., & Mace, G. M. (2000). Predicting extinction risk in declining species. *Proceedings of the Royal Society of London. Series B: Biological Sciences*, *267*(1456), 1947–1952. doi:10.1098/rspb.2000.1234

Ripa, J. & Ives, A. R. (2003). Food web dynamics in correlated and autocorrelated environments. *Theoretical Population Biology*. Understanding the role of environmental vatiation in population and community dynamics, *64*(3), 369–384. doi:10.1016/S0040-5809(03)00089-3

Rooney, N., McCann, K. S., Gellner, G., & Moore, J. C. (2006). Structural asymmetry and the stability of diverse food webs. *Nature*, *442*(7100), 265–269. doi:10.1038/nature04887

Rooney, N., McCann, K. S., & Moore, J. C. (2008). A landscape theory for food web architecture. *Ecology Letters*, *11*(8), 867–881. doi:10.1111/j.1461-0248.2008.01193.x

Shanafelt, D. W. & Loreau, M. (2018). Stability trophic cascades in food chains. *Royal Society Open Science*, *5*(11), 180995. doi:10.1098/rsos.180995

Tscharntke, T., Tylianakis, J. M., Rand, T. A., Didham, R. K., Fahrig, L., Batáry, P., ... Westphal, C. (2012). Landscape moderation of biodiversity patterns and processes - eight hypotheses. *Biological Reviews*, *87*(3), 661–685. doi:10.1111/j.1469-185X.2011.00216.x

Vadeboncoeur, Y., McCann, K. S., Zanden, M. J. V., & Rasmussen, J. B. (2005). Effects of multi-chain omnivory on the strength of trophic control in lakes. *Ecosystems*, *8*(6), 682–693. doi:10.1007/s10021-003-0149-5

Vander Zanden, M. J. & Vadeboncoeur, Y. (2002). Fishes as integrators of benthic and pelagic food webs in lakes. *Ecology*, *83*(8), 2152–2161. doi:10.1890/0012-9658(2002)083[2152:FAIOBA]2.0.CO;2

Vasseur, D. A. & Fox, J. W. (2007). Environmental fluctuations can stabilize food web dynamics by increasing synchrony. *Ecology Letters*, *10*(11), 1066–1074. doi:10.1111/j.1461-0248.2007.01099.x

Vasseur, D. A. & Fox, J. W. (2009). Phase-locking and environmental fluctuations generate synchrony in a predator–prey community. *Nature*, *460*(7258), 1007–1010. doi:10.1038/nature08208

Wang, S., Haegeman, B., & Loreau, M. (2015). Dispersal and metapopulation stability. *PeerJ*, *3*, e1295. doi:10.7717/peerj.1295

Ward, C. L., McCann, K. S., & Rooney, N. (2015). HSS revisited: Multi-channel processes mediate trophic control across a productivity gradient. *Ecology Letters*, *18*(11), 1190–1197. doi:10.1111/ele.12498

Wolkovich, E. M., Allesina, S., Cottingham, K. L., Moore, J. C., Sandin, S. A., & de Mazancourt, C. (2014). Linking the green and brown worlds: The prevalence and effect of multi-channel feeding in food webs. *Ecology*, 140531172126004. doi:10.1890/13-1721.1

Wollrab, S., Diehl, S., & De Roos, A. M. (2012). Simple rules describe bottom-up and top-down control in food webs with alternative energy pathways. *Ecology Letters*, *15*(9), 935–946. doi:10.1111/j.1461-0248.2012.01823.x

Zelnik, Y. R., Arnoldi, J.-F., & Loreau, M. (2019). The three regimes of spatial recovery. *Ecology*, *100*(2), e02586. doi:10.1002/ecy.2586

Zou, K., Thébault, É., Lacroix, G., & Barot, S. (2016). Interactions between the green and brown food web determine ecosystem functioning. *Functional Ecology*, *30*(8), 1454–1465. doi:10.1111/1365-2435.12626

Synchrony and perturbation transmission in trophic metacommunities

Pierre Quévreux[1], Matthieu Barbier[1], and Michel Loreau[1]

[1] *Theoretical and Experimental Ecology Station, CNRS UMR 5321, 09200 Moulis, France*

corresponding author: pierre.quevreux@cri-paris.org

S1 Complementary material and methods

S1-1 Parameters

Table S1-1: Table of parameters. Only combinations of m and a leading to the desired values of ma were kept.

parameter	interpretation	value
σ	standard deviation of stochastic noise	$\{10^{-3}, 10^{-5}\}$
g	net growth rate of primary producers	1
r	death rate of consumers	0
D	self regulation	1
ϵ	conversion efficiency	0.65
m	predator/prey metabolic rate ratio	$\{0.0065, 0.065, 0.65, 6.5, 65\}$
a	attack rate	$\{1/6.5, 1/0.65, 1/0.065\}$
ϵa	positive effect of prey on predators	$\{0.1, 1, 10\}$
ma	negative effect of predators on prey	$\{0.1, 1, 10\}$
d_i	scaled dispersal rate	$[10^{-5}, 10^{5}]$

Table S1-2: Distribution of m and a leading to the desired values of ma and ϵa.

	$\epsilon a = 0.1$	$\epsilon a = 1$	$\epsilon a = 10$
$ma = 10$	$m = 65$ $a = 0.15$	$m = 6.5$ $a = 1.5$	$m = 0.65$ $a = 15$
$ma = 1$	$m = 6.5$ $a = 0.15$	$m = 0.65$ $a = 1.5$	$m = 0.065$ $a = 15$
$ma = 0.1$	$m = 0.65$ $a = 0.15$	$m = 0.065$ $a = 1.5$	$m = 0.0065$ $a = 15$

S1-2 Scaling of biological rates with metabolism

In this study, we extend the model of Barbier and Loreau (2019) where biological rates scale with metabolisms as in many previous studies (Yodzis and Innes, 1992; Brose et al., 2006; Heckmann et al., 2012; Schneider et al., 2016; Quévreux et al., 2020). The scaling of biological rates such as growth rate or mortality rate is well documented (Brown et al., 2004; Savage et al., 2004; Rall et al., 2012) and provide an efficient way to parametrise food web models (Hudson and Reuman, 2013). However, the description of intraspecific interactions (D_i in our model) remains quasi inexistent although its existence and impacts on trophic dynamics and species coexistence have been clearly identified (Barabás et al., 2017; Barbier and Loreau, 2019; Picoche and Barraquand, 2019, 2020; Aubier, 2020). Two main arguments support

the scaling of the density dependent mortality rate D_i with species metabolic rate m_i, one mechanistic, another more mathematical.

From a mechanistic point of view, all biological rates are linked to metabolism as they need energy expenditure, thus it is reasonable to make self-regulation to scale with metabolism. In fact, even if interspecific and intraspecific interactions represent different biological processes, they rely on individuals encounters while they are moving in their environment. As mobility and home range scale with body mass (Pawar et al., 2012, 2019; Carbone et al., 2014; Tamburello et al., 2015; Hirt et al., 2017) such as metabolism, and as movement is linked to energy expenditure, we can reasonably assume that the density dependent mortality rate D_i scales with species metabolic rate m_i.

More mathematically, the main implication of not scaling D_i in the same way as other rates is that smaller or larger species would then exhibit systematically much stronger or much weaker density-dependence, relative to their baseline mortality. There is no clear reason to assume such a systematic bias a priori. Cases of mainly density-dependent or independent mortality have been proposed for both very small and very large (or very fast and slow) species. Thus, we would rather expect unbiased variation between species within the same size or metabolism class, around a general trend of proportional rates.

S1-3 Demographic and environmental perturbations

This section summarises the demonstration of the scaling of demographic and environmental perturbations with species abundance (see Lande et al., 2003 for more details).

The growth of a population depends on the fitness w_i of each individual i. This fitness can be decomposed into the expected fitness μ_w of the species depending on environmental conditions and the individual deviation δ_i. The expected value of w_i is equal to μ_w ($E(w_i) = \mu_w$ and $E(\delta_i) = 0$).

$$w_i = \mu_i + \delta_i \tag{11}$$

Then, the growth rate λ of the population, which contains N individuals, is the mean of the w_i.

$$\lambda = \overline{w} = \frac{1}{N}\sum_{i=1}^{N} w_i = \mu_w + \frac{1}{N}\sum_{i=1}^{N} \delta_i \tag{12}$$

μ_w and δ_i are independent random variables whose variance are respectively σ^2_{env} and σ^2_{demo}. Thus, we can calculate the variance of λ.

$$Var(\lambda) = Var(\mu_w) + Var(\frac{1}{N}\sum_{i=1}^{N} \delta_i) = \sigma^2_{env} + \frac{1}{N^2}\sum_{i=1}^{N} \sigma^2_{demo} = \sigma^2_{env} + \frac{\sigma^2_{demo}}{N} \tag{13}$$

As the growth of the population is defined by λN, we get

$$Var(\lambda N) = N^2 Var(\lambda) = \sigma^2_{env} N^2 + \sigma^2_{demo} N \tag{14}$$

Thus, the variance of the population due to a synchronised response of all the individuals is equal to $\sigma^2_{env} N^2$ while the variance of the demographic noise is equal to $\sigma^2_{demo} N$. In conclusion, we can represent the demographic perturbation by $\sigma_{demo} B^{0.5} dW$ and the environmental perturbation by $\sigma_{env} B dW$ as in equation (5) in the main text.

S1-4 Biomass at equilibrium

The system of equations (4a) and (4b) at equilibrium cannot be solved analytically. Therefore, we calculate analytically the equilibrium biomass of the system without dispersal by solving the following equations:

$$0 = \frac{g}{D} - B_1^* - maB_2^* \tag{15a}$$

$$0 = -\frac{r}{D} - B_i^* + \epsilon a B_{i-1}^* - maB_{i+1}^* \tag{15b}$$

This can be expressed as a matrix product:

$$\begin{pmatrix} -1 & -ma & & (0) \\ \epsilon a & -1 & \ddots & \\ & \ddots & \ddots & -ma \\ (0) & & \epsilon a & -1 \end{pmatrix} \begin{pmatrix} B_1^* \\ B_2^* \\ \vdots \\ B_n^* \end{pmatrix} = \begin{pmatrix} -g/D \\ r/D \\ \vdots \\ r/D \end{pmatrix} \tag{16}$$

solved by the tridiagonal solver algorithm of the GNU Scientific Library version 2.5 (Galassi, 2009). Then, these values initialise the multidimensional root-finder algorithm of the GNU Scientific Library version 2.5 (Galassi, 2009) that solve the following system to find the equilibrium biomasses of the metacommunity.

$$0 = B_1(\frac{g}{D} - B_1 - maB_2) + d_i(B_1' - B_1) \tag{17a}$$

$$0 = B_i(-\frac{r}{D} - B_i + \epsilon aB_{i-1} - maB_{i+1}) + d_i(B_i' - B_i) \tag{17b}$$

These equations have the same solutions that equations (4a) and (4b) but the absence of m_{i-1}, which can be very low or high depending on the value of m, greatly increases the precision of the algorithm.

S1-5 Jacobian matrix

The general system with S species is defined by:

$$\frac{dB_i}{dt} = f_i(B_1, ..., B_S) \tag{18}$$

B^* defines the equilibrium at which the community matrix (or Jacobian matrix) J is defined by:

$$J = \begin{pmatrix} \left.\frac{\partial f_i^{(1)}}{\partial B_j^{(1)}}\right|_{B^*} & \left.\frac{\partial f_i^{(1)}}{\partial B_j^{(2)}}\right|_{B^*} \\ \left.\frac{\partial f_i^{(2)}}{\partial B_j^{(1)}}\right|_{B^*} & \left.\frac{\partial f_i^{(2)}}{\partial B_j^{(2)}}\right|_{B^*} \end{pmatrix} \tag{19}$$

Where $\left.\frac{\partial f_i^{(k)}}{\partial B_j^{(\ell)}}\right|_{B^*}$ represents the effect of species j from patch ℓ on dynamics of species i from patch k. For simplicity, J can be split into blocks such as:

$$J = J' + P' = \begin{pmatrix} J^{(1)} & 0 \\ 0 & J^{(2)} \end{pmatrix} + \begin{pmatrix} -P & P \\ P & -P \end{pmatrix} \tag{20}$$

With $J^{(k)}$ the Jacobian matrix of community k without dispersal and P the sub-dispersal matrix. P is defined by:

$$P = \begin{pmatrix} Dd_1 & & (0) \\ & \ddots & \\ (0) & & m^{n-1}Dd_n \end{pmatrix} \tag{21}$$

And $J^{(k)}$ by:

$$\begin{aligned} J_{11}^{(k)} &= D(\frac{g}{D} - 2B_1^{(k)*} - maB_2^{(k)*}) & J_{12}^{(k)} &= D(-maB_1^{(k)*}) \\ J_{i,i-1}^{(k)} &= m^{i-1}D(\epsilon aB_i^{(k)*}) & J_{i,i+1}^{(k)} &= m^{i-1}D(-maB_i^{(k)*}) \\ J_{i,i}^{(k)} &= m^{i-1}D(-\frac{r}{D} - 2B_i^{(k)*} + \epsilon aB_{i-1}^{(k)*} - maB_{i+1}^{(k)*}) & & \\ J_{i,j}^{(k)} &= 0 \ \text{ if } \ j \notin \{i-1, i, i+1\} & & \end{aligned} \tag{22}$$

S1-6 Linearisation of the system and resolution of the Lyapunov equation

S1-6-1 Linearisation of the system

The system of equations (4a) and (4b) can be linearised in the vicinity of B^*:

$$\frac{dB_i}{dt} = \underbrace{f_i(B_1^*, ..., B_S^*)}_{=0} + \sum_{j=1}^{S} \left(\left.\frac{\partial f_i}{\partial B_j}\right|_{B^*} (B_j - B_j^*) \right) \tag{23}$$

Thus, by setting $X_i = B_i - B_i^*$ the deviation from equilibrium, we have:

$$\frac{dX_i}{dt} = \sum_{j=1}^{S} J_{ij}X_j \tag{24}$$

Then, we can consider small perturbations defined by $\overrightarrow{E}$ whose effects on $\overrightarrow{X}$ are defined by the matrix T (Arnoldi et al., 2016). We get the linearised version of equation (5):

$$\frac{d\overrightarrow{X}}{dt} = J\overrightarrow{X} + T\overrightarrow{E} \tag{25}$$

The elements of $\overrightarrow{E}$ are defined by stochastic perturbations $E_i = \sigma_i dW_i$ with σ_i their standard deviation and dW_i a white noise term with mean 0 and variance 1. In this study, each species can receive three types of perturbation scaling with each biomass (B_i^{*z}): exogenous if $z = 0$, demographic if $z = 0.5$ and environmental if $z = 1$ (see section S1-3). Thus, $\overrightarrow{E} = (E_{1,exo}, ..., E_{S,exo}, E_{1,demo}, ..., E_{S,demo}, E_{1,env}, ..., E_{S,env})$ as it contains the white noise term of each type of perturbation for each species. T contains three blocks of diagonal matrices of size S corresponding to each type of perturbation.

$$T = \begin{pmatrix} 1 & & 0 & B_1^{*0.5} & & 0 & B_1^{*} & & 0 \\ & \ddots & & & \ddots & & & \ddots & \\ 0 & & 1 & 0 & & B_S^{*0.5} & 0 & & B_S^{*} \end{pmatrix} \tag{26}$$

$$\underbrace{\qquad}_{\text{exogenous}} \quad \underbrace{\qquad}_{\text{demographic}} \quad \underbrace{\qquad}_{\text{environmental}}$$

Thus, the matrix product $T\overrightarrow{E}$ results in the product of the white noise and the biomass scaling as in equations (4a) and (4b) in the main text. Moreover, each species can receive simultaneously one perturbation of each type.

S1-6-2 Resolution of the Lyapunov equation

In the vicinity of equilibrium, the Lyapunov equation links the variance-covariance matrix V_E of the perturbation vector $\overrightarrow{E}$ to the variance-covariance matrix C^* of species biomasses (see the appendix of Wang et al. (2015) for more details on the Lyaponov equation).

$$JC^* + C^*J^\top + TV_ET^\top = 0 \tag{27}$$

The diagonal elements of V_E are equal to σ_i^2 (variance of the white noises) and the non-diagonal elements are equal to zero if perturbations are independent (what we consider in this study). $\top$ is the transpose operator.

$$V_E = \begin{pmatrix} \sigma_{1,exo} & & 0 & & & \cdots & & & 0 \\ & \ddots & & \ddots & & & & & \\ 0 & & \sigma_{S,exo} & & \ddots & & & & \\ & \ddots & & \sigma_{1,demo} & & 0 & & & \vdots \\ & & \ddots & & \ddots & & \ddots & & \\ \vdots & & & 0 & & \sigma_{S,demo} & & \ddots & \\ & & & & \ddots & & \sigma_{1,env} & & 0 \\ & & & & & \ddots & & \ddots & \\ 0 & & & \cdots & & & 0 & & \sigma_{S,env} \end{pmatrix} \begin{matrix} \\ \\ \\ \\ \\ \\ \\ \\ \end{matrix} \begin{matrix} \} \text{exogenous} \\ \\ \\ \} \text{demographic} \\ \\ \\ \} \text{environmental} \\ \\ \\ \end{matrix} \tag{28}$$

C^* can be calculated using a Kronecker product (Nip et al., 2013). The Kronecker product of an $m \times n$ matrix A and a $p \times q$ matrix B denoted $A \otimes B$ is the $mp \times nq$ block matrix given by:

$$A \otimes B = \begin{pmatrix} a_{11}B & \cdots & a_{1n}B \\ \vdots & \ddots & \vdots \\ a_{m1}B & \cdots & a_{mn}B \end{pmatrix}$$

We define C_s^* and $(TV_ET^\top)_s$ the vectors stacking the columns of C^* and $TV_ET^\top$ respectively. Thus, equation (27) can be rewrite as:

$$\begin{aligned} (J \otimes I + I \otimes J)C_s^* &= -(TV_ET^\top)_s \\ C_s^* &= -(J \otimes I + I \otimes J)^{-1}(TV_ET^\top)_s \end{aligned} \tag{29}$$

S1-7 Numerical resolution of stochastic differential equations

The same results can be obtained by simulating the temporal dynamics of the system. Equation (5) in the main text can be solved by using the Euler-Maruyama method by computing the discretised equation:

$$B_{i_{t+\Delta t}} = B_{i_t} + f(\overrightarrow{B_t})\Delta t + \sqrt{\Delta t}\sigma_i B_i^z \Delta W_i \tag{30}$$

With Δt the time step and ΔW_i a displacement drawn from a Gaussian distribution with 0 mean and variance 1.

References

Arnoldi, J., Loreau, M., & Haegeman, B. (2016). Resilience, reactivity and variability: A mathematical comparison of ecological stability measures. *Journal of Theoretical Biology*, *389*, 47–59. doi:10.1016/j.jtbi.2015.10.012

Aubier, T. G. (2020). Positive density dependence acting on mortality can help maintain species-rich communities. *eLife*, *9*, e57788. doi:10.7554/eLife.57788

Barabás, G., Michalska-Smith, M. J., & Allesina, S. (2017). Self-regulation and the stability of large ecological networks. *Nature Ecology & Evolution*, *1*(12), 1870–1875. Number: 12 Publisher: Nature Publishing Group. doi:10.1038/s41559-017-0357-6

Barbier, M. & Loreau, M. (2019). Pyramids and cascades: A synthesis of food chain functioning and stability. *Ecology Letters*, *22*(2), 405–419. doi:10.1111/ele.13196

Brose, U., Williams, R. J., & Martinez, N. D. (2006). Allometric scaling enhances stability in complex food webs. *Ecology Letters*, *9*(11), 1228–1236. doi:10.1111/j.1461-0248.2006.00978.x

Brown, J. H., Gillooly, J. F., Allen, A. P., Savage, V. M., & West, G. B. (2004). Toward a metabolic theory of ecology. *Ecology*, *85*(7), 1771–1789. doi:10.1890/03-9000

Carbone, C., Codron, D., Scofield, C., Clauss, M., & Bielby, J. (2014). Geometric factors influencing the diet of vertebrate predators in marine and terrestrial environments. *Ecology Letters*, *17*(12), 1553–1559. doi:10.1111/ele.12375

Galassi, M. (Ed.). (2009). *GNU scientific library: Reference manual* (3. ed., for GSL version 1.12, 1. print). A GNU manual. OCLC: 552301619. s.l.: Network Theory.

Heckmann, L., Drossel, B., Brose, U., & Guill, C. (2012). Interactive effects of body-size structure and adaptive foraging on food-web stability: Body size, adaptivity and food-web stability. *Ecology Letters*, *15*(3), 243–250. doi:10.1111/j.1461-0248.2011.01733.x

Hirt, M. R., Jetz, W., Rall, B. C., & Brose, U. (2017). A general scaling law reveals why the largest animals are not the fastest. *Nature Ecology & Evolution*, *1*(8), 1116–1122. doi:10.1038/s41559-017-0241-4

Hudson, L. N. & Reuman, D. C. (2013). A cure for the plague of parameters: Constraining models of complex population dynamics with allometries. *Proc. R. Soc. B*, *280*(1770), 20131901. doi:10.1098/rspb.2013.1901

Lande, R., Engen, S., & Saether, B.-E. (2003). *Stochastic population dynamics in ecology and conservation*. Oxford University Press. doi:10.1093/acprof:oso/9780198525257.001.0001

Nip, M., Hespanha, J. P., & Khammash, M. (2013). Direct numerical solution of algebraic Lyapunov equations for large-scale systems using Quantized Tensor Trains. In *52nd IEEE Conference on Decision and Control* (pp. 1950–1957). doi:10.1109/CDC.2013.6760167

Pawar, S., Dell, A. I., Lin, T., Wieczynski, D. J., & Savage, V. M. (2019). Interaction dimensionality scales up to generate bimodal consumer-resource size-ratio distributions in ecological communities. *Frontiers in Ecology and Evolution*, *7*. doi:10.3389/fevo.2019.00202

Pawar, S., Dell, A. I., & Savage, V. M. (2012). Dimensionality of consumer search space drives trophic interaction strengths. *Nature*, *486*(7404), 485. doi:10.1038/nature11131

Picoche, C. & Barraquand, F. (2019). How self-regulation, the storage effect, and their interaction contribute to coexistence in stochastic and seasonal environments. *Theoretical Ecology*, *12*(4), 489–500. doi:10.1007/s12080-019-0420-9

Picoche, C. & Barraquand, F. (2020). Strong self-regulation and widespread facilitative interactions in phytoplankton communities. *Journal of Ecology*, 1365–2745.13410. doi:10.1111/1365-2745.13410

Quévreux, P., Barot, S., & Thébault, É. (2020). Interplay between the paradox of enrichment and nutrient cycling in food webs. *Oikos*. in press. doi:https://doi.org/10.1111/oik.07937

Rall, B. C., Brose, U., Hartvig, M., Kalinkat, G., Schwarzmuller, F., Vucic-Pestic, O., & Petchey, O. L. (2012). Universal temperature and body-mass scaling of feeding rates. *Philosophical Transactions of the Royal Society B: Biological Sciences*, *367*(1605), 2923–2934. doi:10.1098/rstb.2012.0242

Savage, V. M., Gillooly, J. F., Woodruff, W. H., West, G. B., Allen, A. P., Enquist, B. J., & Brown, J. H. (2004). The predominance of quarter-power scaling in biology. *Functional Ecology*, *18*(2), 257–282. doi:10.1111/j.0269-8463.2004.00856.x

Schneider, F. D., Brose, U., Rall, B. C., & Guill, C. (2016). Animal diversity and ecosystem functioning in dynamic food webs. *Nature Communications*, *7*, 12718. doi:10.1038/ncomms12718

Tamburello, N., Côté, I. M., & Dulvy, N. K. (2015). Energy and the scaling of animal space use. *The American Naturalist*, *186*(2), 196–211. doi:10.1086/682070

Wang, S., Haegeman, B., & Loreau, M. (2015). Dispersal and metapopulation stability. *PeerJ*, *3*, e1295. doi:10.7717/peerj.1295

Yodzis, P. & Innes, S. (1992). Body size and consumer-resource dynamics. *The American Naturalist*, *139*(6), 1151. doi:10.1086/285380

S2 Complementary results

S2-1 General responses of the food chain model to perturbations

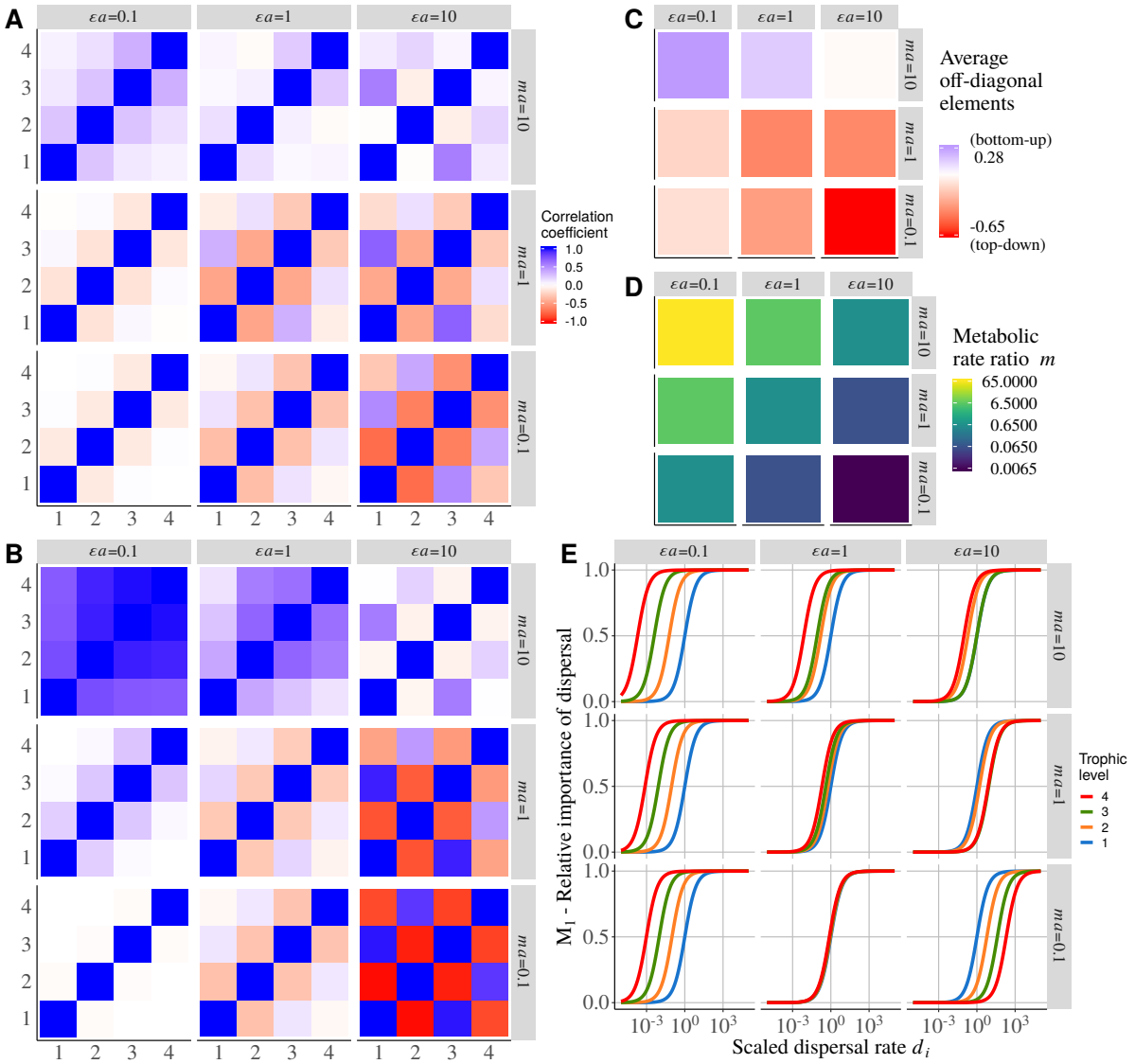

Figure S2-1: **A)** Correlation matrix within an isolated food chain ($d_i = 0$, no dispersal) and with demographic independent stochastic perturbations applied to each trophic level. Nine food chains with different combinations of ϵa and ma are tested. **B)** Same correlation matrix with environmental independent stochastic perturbations applied to each trophic level. **C)** General behaviour of the food chains presented in **A**. All the off-diagonal elements are summed. If the output is positive, correlations are stronger and the food chain has a bottom-up response to perturbations, otherwise, anti-correlations are stronger and the food chain has a top-down response. **D)** Ratio of predator to prey metabolic rates ($m = m_i + 1/m_i$). **E)** M_1, ratio of dispersal processes to the sum demographic and dispersal processes (see equation (9)) for each trophic level along a scaled dispersal rate d_i gradient.

Fig.S2-1 is complementary to Fig.2. In Fig.S2-1A where all species receive independent demographic perturbations, adjacent trophic levels are correlated for $ma = 10$ while they are anti-correlated for $ma \leq 1$ (bottom part of the graph). These two responses correspond respectively to bottom-up and top-down responses of the food chain to perturbations (Fig.S2-1C). Such a difference is not due to biomass distribution among trophic levels as the variance of demographic perturbations is linear to species biomass. This is due to the values of m ($= m_{i+1}/m_i$, ratio of predator to prey metabolic rates, Fig.S2-1D) that is much larger than 1 when the response of the food chain is strongly bottom-up and much lower than 1 when the response is strongly top-down. If predators have a faster metabolic rate than their prey, their demographic dynamics are fast and they recover from perturbations faster than their prey. This makes lower trophic levels relatively more sensitive to perturbations and leads to a bottom-up response

to perturbations. The opposite situation makes predators more sensitive to perturbations and leads to a top-down response.

Environmental perturbations ($z = 1$, see equation (26), Fig.S2-1B) lead to a distribution of bottom-up and top-down responses similar to Fig.S2-1A but with stronger responses in the top-left and bottom-right corners of the graph. In fact, environmental perturbations affect more abundant species and are thus equivalent to demographic perturbations applied to a unique trophic level. Then, Fig.S2-1B is a mix between Fig.2C and 2D depending on biomass distribution (Fig.2A).

Finally, M_1, which is the relative importance of dispersal processes versus demographic processes (Fig.S2-1E), completely depends on biomass distribution (Fig.2A): lower is the biomass, lower is the scaled dispersal rate d_i required to affect species biomass dynamics.

S2-2 Transmission of perturbations to an undisturbed patch

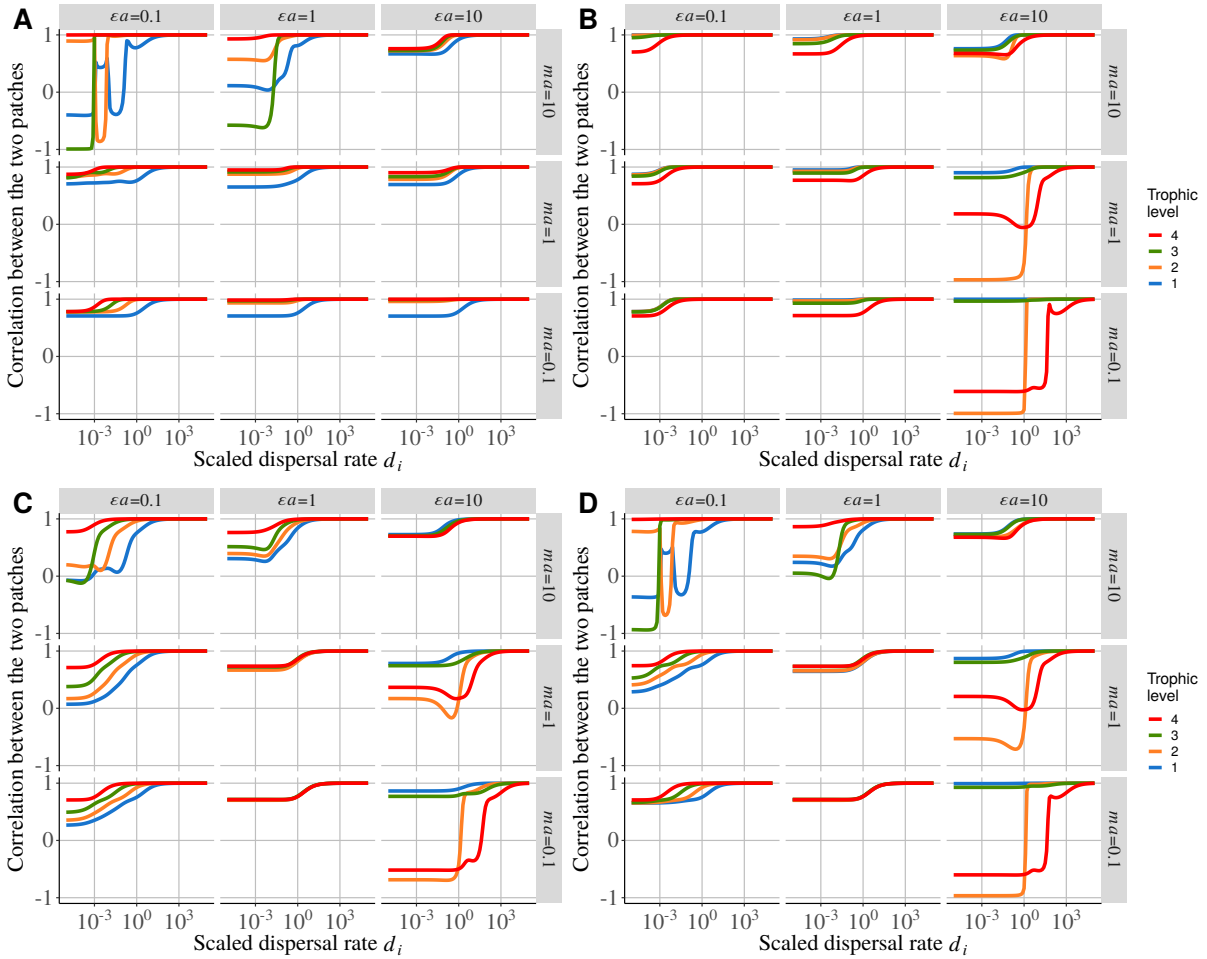

Figure S2-2: Correlation between populations of the same species from two patches with increasing scaled dispersal rates d_i. All species are able to disperse. **A)** Only the primary producer of patch #1 receive a stochastic demographic perturbation. **B)** Only the top predator of patch #1 receive a stochastic demographic perturbation. **C)** All species of patch #1 receive independent stochastic demographic perturbations. **D)** All species of patch #1 receive independent stochastic environmental perturbations.

The top-left corner ($\epsilon a = 0.1$ and $ma = 10$) of Fig.S2-2A, where primary producers in patch #1 are perturbed, was detailed in Fig.4 but the same framework can be used to explain Fig.S2-2A and Fig.S2-2B, where top predators in patch #2 are perturbed, for all other combinations of ϵa and ma. If the perturbed species is also the most affected by dispersal (Fig.S2-1E), then both patches are correlated as the perturbation is transmitted at the same trophic level in patch #2 as it is applied in patch #1 (for $\epsilon a = 10$ in Fig.S2-2A and $\epsilon a = 0.1$ in Fig.S2-2B). In other words, both patches receive almost the same perturbation at the same trophic level. In addition, the same pattern is observed in food chains where all species have the same biomass as they are equally affect by dispersal (Fig.S2-1E).

If the species sensitive to dispersal is not the perturbed one in patch #1, we observe a bottom-up response in one patch and a top-down response in the other one as each patch receives a perturbation at

a different trophic level. This leads to the pattern detailed in Fig.3 and Fig.6. In Fig.S2-2C where all species in patch #1 are perturbed, the top-left corner looks like Fig.S2-2A and the bottom-right corner to Fig.S2-2B. As isolated food chains have respectively bottom-up and a top-down responses in these two parts of the parameter space (Fig.S2-1C), we can indeed expect responses similar to those where primary producers (Fig.S2-2A) and top predators (Fig.S2-2A) are respectively perturbed.

Finally, Fig.S2-2D, where all species in patch #1 receive environmental perturbations, is a mix between Fig.S2-2A and Fig.S2-2B as biomass distribution biases the effect of environmental perturbations towards the more abundant species. Thus, environmental perturbations in bottom-heavy biomass pyramids are equivalent to a perturbation of primary producers (top-left corner and Fig.S2-2A) while in top-heavy biomass pyramids they are equivalent to a perturbation of top predators (bottom-right corner and Fig.S2-2B).

S2-3 Multiple perturbation partitioning

S2-3-1 Mathematical demonstration of correlation partitioning

We consider R independent stochastic perturbations that can affect species from patch #1 or patch #2. Therefore, the variance-covariance matrix of stochastic perturbations V_E is a diagonal matrix whose elements are equal to the variance σ_j^2 of each perturbation j. Thus, we define V_{Ej} the variance-covariance matrix when only the j^{th} perturbation is applied and we have $V_E = \sum_{j=1}^{R} V_{Ej}$.
From equation (29) we have:

$$\begin{aligned} C_s^* &= -(J \otimes I + I \otimes J)^{-1}(TV_E T^\top)_s \\ &= -(J \otimes I + I \otimes J)^{-1}(T \sum_{j=1}^{R} V_{Ej} T^\top)_s \\ &= \sum_{j=1}^{R} \left(-(J \otimes I + I \otimes J)^{-1}(TV_{Ej}T^\top)_s\right) \\ &= \sum_{j=1}^{R} C_{s,j}^* \end{aligned} \tag{31}$$

$C_{s,j}^*$ is the variance-covariance matrix associated to V_{Ej}. Thus, we have:

$$w_{i^{(k)}m^{(\ell)}} = \sum_{j=1}^{R} w_{i^{(k)}m^{(\ell)},j} \tag{32}$$

$w_{i^{(k)}j^{(\ell)}}$ is the covariance between species i in patch k and species j in patch ℓ and is an element of the variance-covariance matrix C^* and $w_{i^{(k)}m^{(\ell)},j}$ is an element of the variance-covariance matrix C_j^*. As we only consider two patches and are interested in the correlation between populations of the same species, we use the following notation:

$$w_{1,j} = w_{i^{(1)}i^{(1)},j} \qquad w_{2,j} = w_{i^{(2)}i^{(2)},j} \qquad w_{1,2,j} = w_{i^{(1)}i^{(2)},j}$$

We also define ρ_i that is the correlation coefficient between the two populations of species i and $\rho_{i,j}$ in the same correlation coefficient in the case where only the j^{th} perturbation is applied.

$$\begin{aligned} \rho_i = \frac{w_{1,2}}{\sqrt{w_1 w_2}} &= \frac{\sum_{j=1}^{R} w_{1,2,j}}{\sqrt{\sum_{k=1}^{R} w_{1,k}}\sqrt{\sum_{k=1}^{R} w_{2,k}}} \\ &= \frac{\sum_{j=1}^{R} \rho_{i,j}\sqrt{w_{1,j}w_{2,j}}}{\sqrt{\sum_{k=1}^{R} w_{1,k}}\sqrt{\sum_{k=1}^{R} w_{2,k}}} \end{aligned} \tag{33}$$

$$= \sum_{j=1}^{R} \left(\rho_{i,j} \frac{\sqrt{w_{2,j}}}{\sqrt{w_{1,j}}} \frac{w_{1,j}}{\sqrt{\sum_{k=1}^{R} w_{1,k}} \sqrt{\sum_{k=1}^{R} w_{2,k}}} \right)$$

Eventually, the correlation pattern (ρ_i) in a metacommunity where all species receive independent stochastic perturbations can be decomposed into a sum of the correlation patterns ($\rho_{i,j}$) obtained when only one species is perturbed. The the $\rho_{i,j}$ are weighted by the variance generated in both patches by each perturbation.

S2-3-2 Verification for the whole parameter space

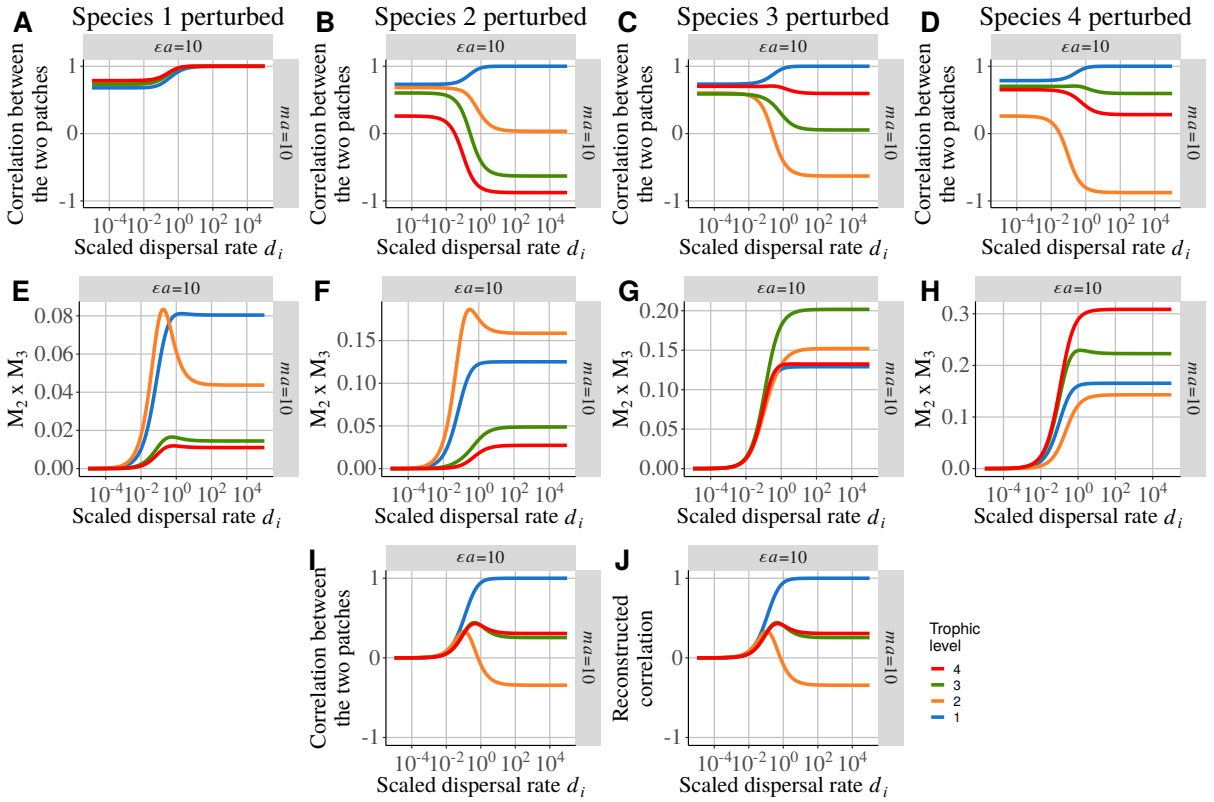

Figure S2-3: Detailed correlation pattern between two coupled food chains for $\epsilon a = 10$ and $ma = 10$ with increasing scaled dispersal rates d_i. Only primary producers are able to disperse. **A)**, **B)**, **C)** and **D)** are the correlation patterns between the two patches and **E)**, **F)**, **G)** and **H)** are the products of the two metric M_2 and M_3 when species 1, 2, 3 and 4 are respectively the only species perturbed. **I)** Correlation between patches when independent demographic stochastic perturbations are applied to all species in each patch. **J)** Reconstructed correlation pattern when all species in each patch are perturbed. It can by obtained as follow: **J**= 2×(**A**×**E**+**B**×**F**+**C**×**G**+**D**×**H**).

The results found with a food chain sustaining four trophic levels (Fig.S2-3) are consistent with the results from a food chain two with trophic levels (Fig.6). Primary producer populations become completely correlated as they are the only species able to disperse. Perturbing herbivores (Fig.S2-3F), carnivores (Fig.S2-3G) and top predators (Fig.S2-3H) generates at least three times more variability in herbivore biomass than perturbing primary producers (Fig.S2-3E). Thus, the average of the correlation patterns between herbivore populations in Fig.S2-3B-D gives the moderated anti-correlation seen in Fig.S2-3I and S2-3J.

Carnivores are mostly and equally affected by the perturbation of carnivores (Fig.S2-3G) and top predators (Fig.S2-3H). Thus, averaging the corresponding correlation patterns (Fig.S2-3C andS2-3D) leads to the moderated correlation between the two carnivore populations (Fig.S2-3I and S2-3J).

Finally, top predators variability is mostly driven by their direct perturbation (Fig.S2-3H), making the corresponding correlation pattern (Fig.S2-3D) very similar to the correlation pattern obtained with

multiple perturbations (Fig.S2-3I and S2-3J).

The partitioning of the effects of perturbations is also valid for the rest of the parameter space (Fig.S2-4A and S2-4B) and when only top predators are able to disperse (Fig.S2-4C and S2-4D) or when all species are able to disperse (Fig.S2-4E and S2-4F).

S2-4 Environmental perturbations

Finally, we explore the effect of independent environmental perturbations ($z = 1$, see equation (26)) applied to all species in patch #1 in addition to demographic perturbations applied to all species in both patches. We test two ratios of environmental to demographic variances ($\sigma^2_{env} : \sigma^2_{demo}$) to understand how environmental perturbations can override the background demographic perturbations. Thus, we compare the variance generated in patch #2 when only environmental perturbations are applied in patch #1 to the variance generated when species from both patches receive independent demographic perturbations only.

Weak environmental perturbations ($\sigma^2_{env} : \sigma^2_{demo} = 0.001$) have no effects as Fig.S2-5A is identical to Fig.S2-4E (patch #1 and #2 receiving independent demographic perturbations only). At low scaled dispersal rates d_i, the variability due to the environmental perturbations transmitted to patch #2 through dispersal is completely overwhelmed by the variability due to demographic perturbations directly affecting species in patch #2 (Fig.S2-5B). The increase in the transmitted variability from environmental perturbations at high scaled dispersal rates is also jointed by the strong correlation of populations due to dispersal (Fig.S2-2D). This increased correlation between patches due to dispersal overrides the increasing influence of environmental perturbations as all populations become completely coupled (bottom-right graph of Fig.S2-5B).

However, strong environmental perturbations ($\sigma^2_{env} : \sigma^2_{demo} = 100$) have dominant effects at intermediate scaled dispersal rates as Fig.S2-5C is similar to Fig.S2-2D. At low scaled dispersal rates d_i, the variance ratio is low and patches remain uncorrelated (Fig.S2-5D) while at high scaled dispersal rates, populations are perfectly correlated. Food chains with top-heavy biomass pyramids (Fig.2A) seem particularly affected by environmental perturbations. Thus, changes of scaled dispersal rates can dramatically switch population from anti-correlation to correlation.

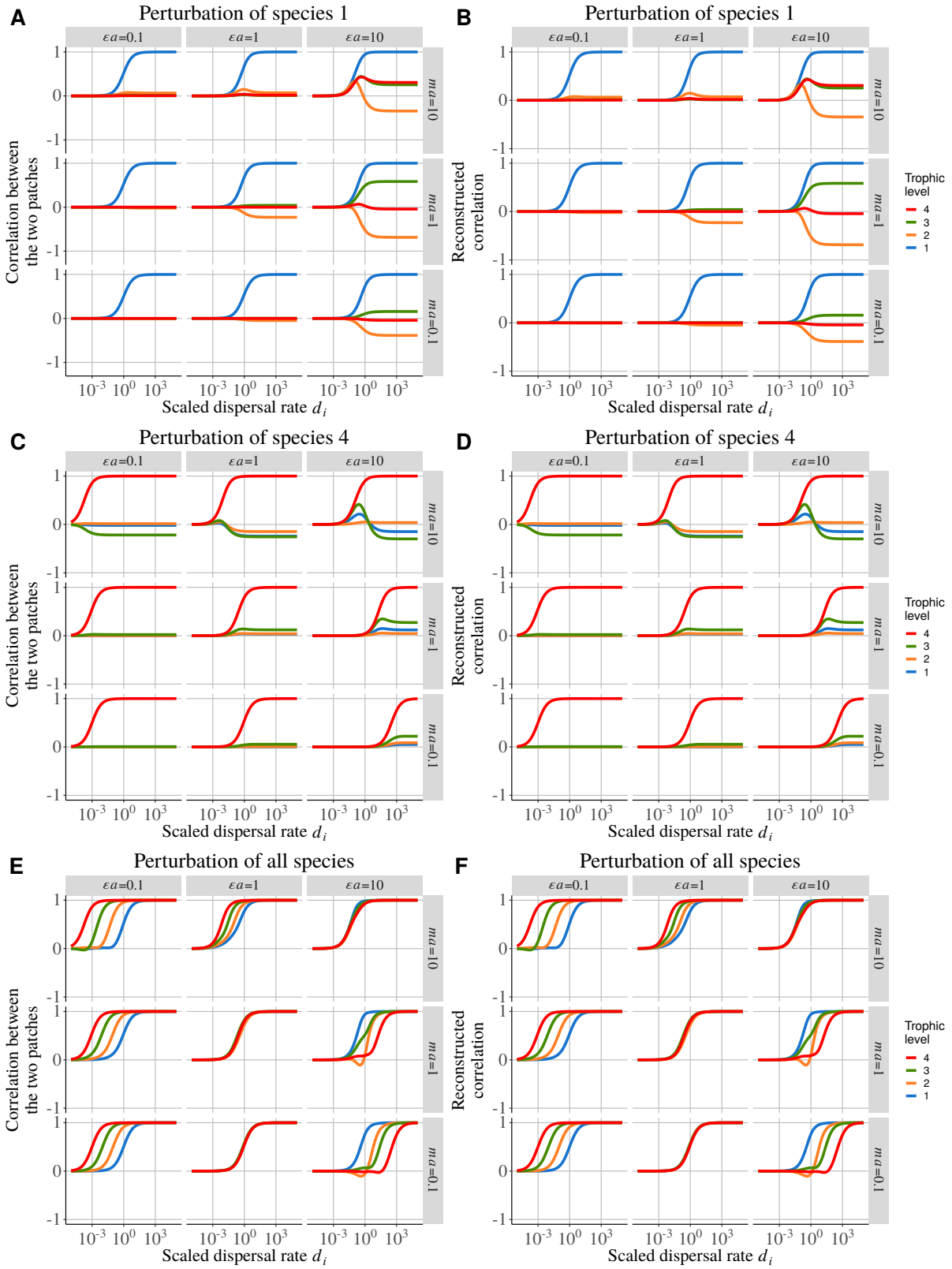

Figure S2-4: Correlation between populations of the same species from two patches with increasing scaled dispersal rates d_i. Independent demographic stochastic perturbations are applied to each species in each patch. **A)** Only primary producers are able to disperse. **C)** Only top predators are able to disperse. **E)** All species are able to disperse. Reconstructed correlation pattern when all species in each patch are perturbed. The reconstruction process is the same as explained in Fig.6 and Fig.S2-3 but applied to the whole parameter space and for the cases where **B)** only primary producers **D)** only top predators are able to disperse and **F)** all species are able to disperse.

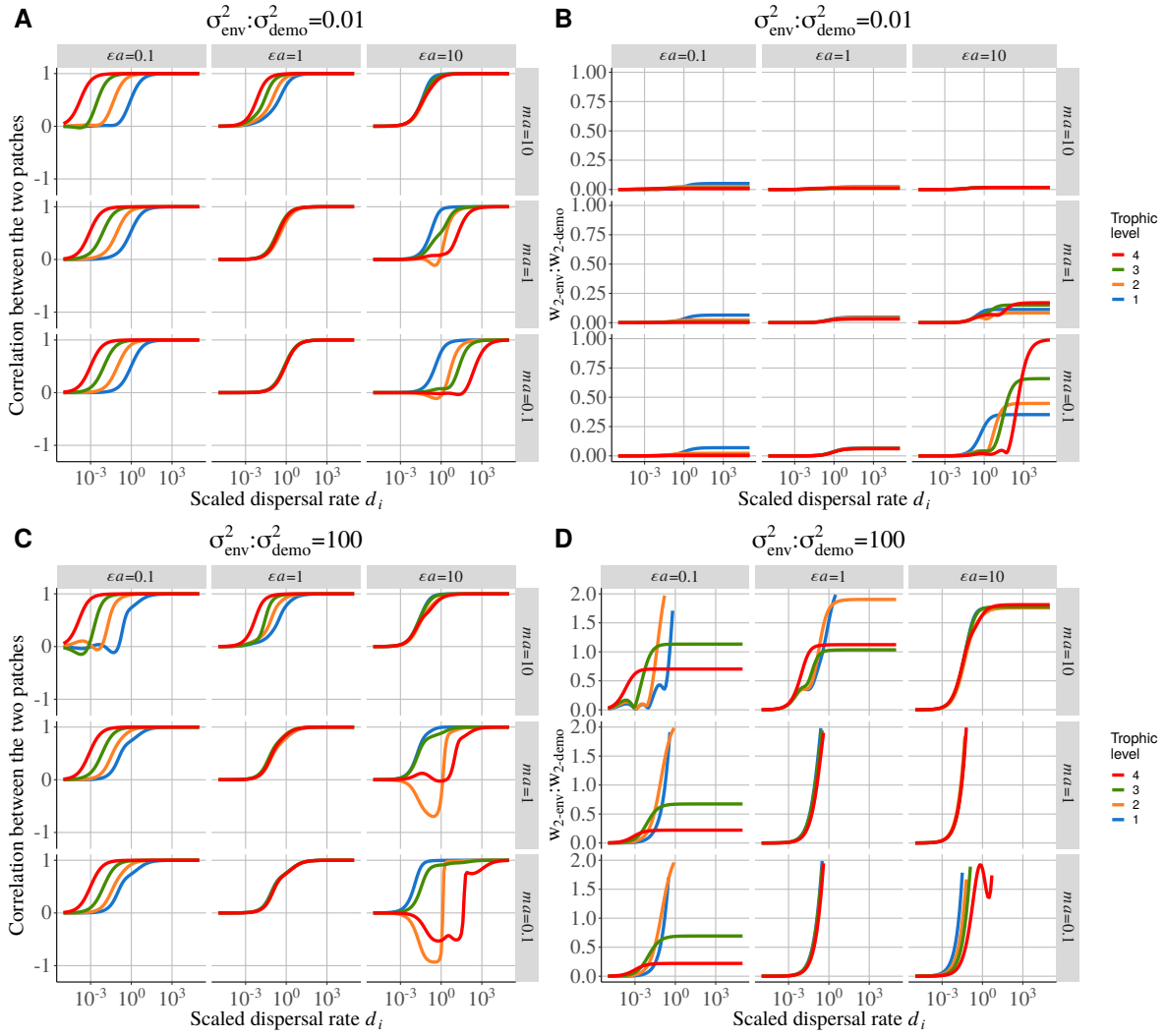

Figure S2-5: Correlation between populations of the same species from two patches with increasing scaled dispersal rates d_i. Independent demographic stochastic perturbations are applied to each species of each patch and independent environmental perturbations are applied to each species of patch #1. The relative weight of these two perturbations is given by the ratios of variance w_{2-env} in patch #2 when only species in patch #1 receive independent environmental perturbations to the variance w_{2-demo} in patch #2 when all species receive independent demographic perturbations. Two different ratios of environmental perturbation to demographic perturbation variance are tested: **A)** correlation and **B)** biomass CV ratio for $\sigma^2_{env} : \sigma^2_{demo} = 0.01$ (stronger demographic perturbation) and **C)** correlation and **D)** biomass CV ratio (y-axis cut for more readability) for $\sigma^2_{env} : \sigma^2_{demo} = 100$ (stronger environmental perturbation).